**Article:**

Chen, X, Li, F, Jia, B et al. (3 more authors) (2021) Optimizing storage location assignment in an automotive Ro-Ro terminal. Transportation Research Part B: Methodological, 143. pp. 249-281. ISSN 0191-2615

https://doi.org/10.1016/j.trb.2020.10.009

Please cite the paper as:
Chen X, Li F, Jia B, Wu J, Gao Z and Liu R (2021) Optimizing storage location assignment in an automotive Ro-Ro terminal. **Transportation Research Part B,** 143, 249-281. doi.org/10.1016/j.trb.2020.10.009

# Optimizing storage location assignment in an automotive Ro-Ro terminal

Xiaojing Chen, Feng Li[1]
State Key Laboratory of Rail Traffic Control and Safety, Beijing Jiaotong University, Beijing, 100044, China
Bin Jia[2]
Institute of Transportation System Science and Engineering, Beijing Jiaotong University, Beijing 100044, China
Jianjun Wu
State Key Laboratory of Rail Traffic Control and Safety, Beijing Jiaotong University, Beijing, 100044, China
Ziyou Gao
Institute of Transportation System Science and Engineering, Beijing Jiaotong University, Beijing 100044, China
Ronghui Liu
Institute for Transport Studies, University of Leeds, Leeds LS2 9JT, United Kingdom

**Abstract:** Automotive roll-on/roll-off (Ro-Ro) transportation is an efficient and competitive method for the large-scale transshipment of commercial cars. However, the low-efficiency operations and insufficient storage resources of automotive Ro-Ro terminals have constrained the development of Ro-Ro transportation. This paper investigates the storage location assignment problem (SLAP) for the arrival of cars at the yard, and it aims to improve the ship-loading efficiency and contribute to efficient storage at Ro-Ro terminals. Two deadlock situations resulting from blocked routes are analyzed in detail. Based on the Ro-Ro ship stowage plan, a car group concept is proposed to reflect the loading sequence of cars into a Ro-Ro ship. The dispersion degree is defined to describe the centralized layout of every car group in the yard. A linear 0-1 integer programming model is formulated to minimize the total dispersion degrees of all car groups. Furthermore, an indicator called the attraction degree is presented to quantify the preferred degree of each location for storing different groups of cars. A hierarchical two-stage exchange strategy (HTSES) is designed to obtain the car layout with the minimum total dispersion degree. To reduce the scale of the solved problem, a rolling-horizon heuristic approach based on closed-loop (positive and negative) feedback is proposed. Positive feedback based on the guidance mechanism describes the guidance provided by the existing car layout to arriving cars, while negative feedback based on the reformulation mechanism represents the influence of arriving cars on the car layout. A series of numerical experiments show that the proposed method can effectively produce a satisfactory car assignment

[1] Corresponding author. E-mail: fengli0925@bjtu.edu.cn.

[2] Corresponding author. E-mail: binjia@bjtu.edu.cn.

plan for the management of automotive Ro-Ro terminals.

**Key words:** automotive Ro-Ro terminal; storage location assignment; dispersion degree; attraction degree; rolling horizon

# 1 Introduction

Over the past decade, short sea shipping (SSS) has increasingly been explored as a way to alleviate highway congestion, facilitate trade, improve waterway capacity utilization and reduce greenhouse gas emissions. The European Commission developed the "Motorways of the Sea" (MoS) project to support SSS (Morales-Fusco et al., 2012). In addition to its cost advantage over other transportation modes (Cancı and Erdal, 2003), maritime traffic, including inland water transportation, is considered to be a key element of intermodal transportation for addressing the increasing problems caused by highway and railway congestion and air pollution (Jugovic et al., 2011).

With the development of SSS, roll-on/roll-off (Ro-Ro) transportation has played an increasingly important role in automotive supply chain management (Dias et al., 2010). This specific mode integrates road and maritime transportation and reduces costs in the automotive supply chain. Many ports worldwide, including those at Vigo, Santander, Pasajes, Barcelona, Sagunto, Setúbal, Le Havre, Livorno, Sheerness (Medway ports), Bristol, Copenhagen, Malmö, Göeborg, Emden, Zeebrugge/Ghent, Antwerp, and Rotterdam, have been equipped with Ro-Ro terminals. Figure 1 presents a screenshot of the Shanghai Haitong Ro-Ro Terminal from Google Maps (Google, 2019).


Figure 1 A partial storage region at the Shanghai Haitong Ro-Ro Terminal.

Automotive Ro-Ro terminals are responsible for the storage, loading and unloading of commercial cars (Iannone et al., 2016). Despite their low costs, ports face fierce competition from road and railway transport due to their fewer manual operations and higher efficiency. Low-efficiency operations in Ro-Ro terminals increase the risk of disturbance to ship schedules, and result in port traffic congestion (Maksimavicius, 2004). Regarding tidal harbors, a high ship-loading efficiency is required to avoid ship departure delays. Additionally, unlike shipping containers, commercial cars cannot be stacked in a yard (Iannone et al. 2016). With the increase in commercial cars, limited storage resources have constrained the development of Ro-Ro terminals. For administrators, improving the ship-loading efficiency and the efficient use of storage resources to promote the competitiveness of Ro-Ro terminals is a major challenge.

Unlike ship-loading operations in container terminals, in automotive Ro-Ro terminals, the use of auxiliary equipment—such as quay cranes (QCs), yard cranes (YCs), automated stacking cranes (ASCs) and inner trucks (ITs)—is unnecessary. The loading of commercial cars into ships at Ro-Ro terminals is directly carried out by drivers. Finding storage locations for individual cars as rapidly as possible is very important for ship-loading efficiency; thus, it is beneficial for drivers to spend minimal time searching for loaded cars. Therefore, a rational car layout is more important in Ro-Ro terminals than in container terminals.

In actual yard management, a Ro-Ro terminal will charge suppliers (customers) an extra storage fee once their commodities are stored in the yard for a time exceeding a certain limit. For example, in the Shanghai Haitong Ro-Ro Terminal, if commercial cars are stored at the yard for less than one week, then the storage is free. Hence, commercial cars from different suppliers arrive gradually at the Ro-Ro terminal over the course of one week. The loading operations of cars into a Ro-Ro ship are very intensive.

The yard region of automotive Ro-Ro terminals is usually divided into many zones (Figure 1). Commercial cars that need to leave the port together are usually stored in interconnected parts of the yard (Fischer and Gehring, 2006; Iannone et al., 2016). However, although the cars loaded into the same ship are assigned to one or more adjacent zones, the layout of cars possessing the same ship-loading sequence may still be scattered throughout the selected zone/zones. For instance, Section 3.3 introduces an assignment method based on car type that is applied at the Shanghai Haitong Ro-Ro Terminal. Here, the term “type” reflects a classification of cars based on their suppliers, brands, versions, etc.; its definition is described in detail in Section 3.3. The assignment rule based on car type is simply called “AR-CT”. As shown in Section 3.3, AR-CT leads to a scattered layout corresponding to the loading sequence of cars.

Compared to the operations associated with cars entering the yard, intensive ship-loading operations have higher working efficiency requirements for employees. Based on the ship-loading requirements, one or several teams of drivers are arranged for the loading operations of a Ro-Ro ship. For example, in the Shanghai Haitong Ro-Ro Terminal, 10 drivers will be arranged as a team for the ship-loading operations of approximately 200 cars, and at most three teams of drivers will be employed for the loading operations of a Ro-Ro ship because there are finite human resources. Each team is equipped with a mini-bus for the transfer of drivers from the ship to the yard. For one circular ship-loading operation, employees drive cars from the yard to the Ro-Ro ship and then simultaneously return to the yard via mini-bus. A driver who completes the loading operation will wait at the quay until all other drivers in the team complete their tasks. Once the drivers return to the destination zone, they will walk to find their next cars. Clearly, a rational car layout is advantageous for ship-loading efficiency, which is a pivotal factor reflecting the productivity of a Ro-Ro terminal. For instance, in one circular ship-loading operation, if the cars that will be loaded into the same region of a Ro-Ro ship are assigned to a region of one zone, the time required for drivers to find the cars can be reduced. Moreover, the ideal car layout can strengthen the coordinated operations of drivers in a team and reduce the waiting time of drivers at the quay. In conclusion, a scattered layout will result in a ship-loading process with low efficiency, complicated driver scheduling and congested port traffic.

Additionally, once a car, which is a valuable commodity, is assigned to a storage location, it should remain in the same position before being loaded into a Ro-Ro ship to reduce the risk of damage (no-relocation rule) (Cordeau et al., 2011). A feasible car assignment plan should ensure the availability of a route for cars to enter and exit their assigned locations. The spatial structure of the storage locations in a zone allows cars to enter or exit their assigned storage locations only along the column direction because the transverse movement of cars in the zone is prohibited to avoid damage. In Section 3.3, it is proven that AR-CT can guarantee route availability for cars. However, in AR-CT, an insufficient utilization of yard resources is also found. Hence, if changing the storage strategy based on AR-CT, it is challenging to ensure that there are feasible routes for the cars in a zone.

This paper investigates the storage location assignment problem (SLAP) at an automotive Ro-Ro terminal. In particular, we focus on the assignment of individual cars in one or more selected zones by considering the loading sequence of cars in a Ro-Ro ship. We aim to improve ship-loading efficiency and fully utilize storage resources. A new assignment rule based on the car group, which is simply called "AR-CG", is proposed to develop the centralized car layout associated with the loading sequence of cars. The term "car group" describes a classification indicator of cars based on their loaded regions in a Ro-Ro ship; this definition is explained in detail in Section 3.4. Moreover, an indicator called the dispersion degree is used to quantify the centralized car layout in the selected zone/zones. A linear 0-1 integer programming model is formulated to minimize the total dispersion.

The proposed model aims to avoid deadlock situations caused by blocked routes for arriving and departing cars. Finally, a hierarchical two-stage exchange strategy (HTSES) is designed to obtain the car layout with the minimum dispersion degree, and a rolling-horizon approach based on closed-loop feedback is proposed to identify the spatiotemporal conflicts among cars and to reduce the problem scale.

This paper is organized as follows. Section 2 reviews the literature on yard operations at ports, especially Ro-Ro terminals. In Section 3, we describe the SLAP in detail. The mathematical model is formulated in Section 4. Section 5 illustrates an HTSES based on the attraction degree. A rolling-horizon approach based on closed-loop feedback is proposed in Section 6. Section 7 analyzes numerical experiments in detail. Finally, conclusions are drawn in Section 8.

# 2 Literature review

In addition to the automotive road transportation field (Hu and Sheng, 2014; Vilkelis and Jakovlev 2014; Hu et al., 2015), Ro-Ro transportation has received increasing attention from the automotive supply chain management field. Existing studies tend to focus on the commercial aspects of Ro-Ro transportation (Mangan et al. 2002; Bergantino and Bolis, 2008; Dias et al., 2010). Additionally, scholars have investigated the storage capacity of Ro-Ro terminals (Mattfeld and Orth, 2006; Morales-Fusco et al., 2010; Keceli et al., 2013; Özkan et al., 2016). Regarding optimization models and techniques, little research has focused on automotive Ro-Ro terminals compared to container terminals. Steenken et al. (2004) and Stahlbock and Voß (2008) classified the main logistics processes and operations at container terminals and presented a survey of the related optimization methods. Storage management is an important issue in container terminal operation optimization (Preston and Kozan 2001; Kim and Park 2003; Murty et al., 2005a, 2005b; Guldogan, 2010; Ng et al., 2010; Park et al., 2011; Yu and Qi, 2013; Wu and Zhu, 2015). Additionally, Carlo et al. (2014) comprehensively reviewed the challenges of the current operational paradigms in storage yard operations.

The ship-loading operations at an automotive Ro-Ro terminal are completely different from those at a container terminal. **For a container terminal**, the loading of containers depends on the cooperation among auxiliary equipment, such as QCs, YCs, ASCs, and ITs. Hence, improving the ship-loading efficiency of a container terminal depends on the cooperation between storage space allocation and auxiliary equipment scheduling. Zhang et al. (2003) investigated the storage space allocation problem at container terminals; this problem is related to all the resources in terminal operations, such as QCs, YCs, and ITs. Guldogan (2010) adopted a hierarchical method to handle the assignment of containers and ITs. At the first level, the work balance and the number of trucks were considered, and at the second level, a segregation strategy was proposed to cluster containers based on their departure dates. Lee et al. (2006) investigated the assignment of containers to minimize the total number of gantry crane shifts required to handle complete workloads. Ku et al. (2010) compared several storage space assignment strategies for the scheduling of rail-mounted gantry cranes. Park et al. (2011) discussed the selection of blocks to balance the workloads of ASCs and then analyzed the specific storage assignment based on ASC utilization. Lee et al. (2012a, and 2012b) integrated the decisions for determining the scheduling of feeder vessels and the storage locations of transshipment containers. Additional work has been conducted by Crainic et al. (1993), Cheung and Chen (1998), Shen and Khoong (1995), Laik and Hadjiconstantinou (2008), Han et al. (2008), Jiang et al. (2012), and Sharif and Huynh (2013).

**For an automotive Ro-Ro terminal**, the ship-loading operations of commercial cars do not depend on auxiliary equipment. Commercial cars are moved directly by teams of drivers from the yard to Ro-Ro ships, and each driver team returns to the yard together in one mini-bus for the next ship-loading operation. More focus must be placed on reasonably formulating a car layout in the yard and scheduling drivers to improve ship-loading efficiency. Mattfeld and Kopfer (2003) modeled manpower availability and inventory capacity in vehicle transshipment. A two-stage hierarchical method was presented to solve the complex combinatorial problem. The developed decision system can be applied to potentially integrate customers in the planning process. Fischer and Gehring (2005) developed a multiagent system (MAS) for the integration of storage allocation and deployment scheduling in vehicle transshipment planning. Their randomly generated numerical experiments proved the robustness of the MAS with regard to changes in the data. Cordeau et al. (2011) formulated a yard management problem in an automotive transshipment terminal to minimize the total car handling time. An adaptive neighborhood search metaheuristic was proven to efficiently solve the proposed problem. They proposed the concept of a group in the transfer of cars between the same vessel pair. Unlike in Fischer and Gehring (2005), the delivery destinations of cars were not considered in the classification.

Regarding the storage of cargo in the yard, automotive Ro-Ro and container terminals have different rules. **In container terminals**, the reshuffling or relocation of containers is allowed, although it is detrimental to ship-loading efficiency. Many studies have focused on minimizing the number of reshuffling operations in container terminals (Kim et al., 2000; Kim and Kim, 2002; Kang et al., 2006; Dekker et al., 2006; Borgman et al., 2010; Chen and Lu, 2012; Zeng et al., 2017; Zhou and Zhang, 2018). For example, Kim and Kim (2002) proposed a heuristic rule to minimize the number of relocations during the pickup operation of all containers in a yard bay. Kang et al. (2006) developed a simulated annealing (SA) approach to reduce the number of rehandling operations for export containers with uncertain weight information. Borgman et al. (2010) discussed the trade-off between the travel times of stacking cranes and the probability of reshuffles. In their hierarchical approach, Chen and Lu (2012) focused on avoiding rehandling operations for the assignment of export containers.

However, **in automotive Ro-Ro terminals,** cars are a valuable commodity, and the relocation of cars in the yard should be forbidden to minimize the risk of damage (Cordeau et al. 2011). Hence, a feasible car assignment plan should ensure available routes for cars entering or exiting their storage locations. Fischer and Gehring (2005) allowed the relocation of cars based on a set of buffer areas in the terminal. Although the discussion of route availability is avoided, traffic congestion may occur in the port when many operations occur in the buffer area. AR-CT, presented in Section 1, allows no more than two types of cars to be stored in each column of one zone (Section 3.3), ensuring feasible routes for all cars in one zone; however, this assignment rule does not result in an efficient use of storage resources due to the diversity of car types.

In brief, based on the differences in ship-loading operations between container and automotive Ro-Ro terminals, the distribution of containers in the yard should be neither too centralized nor too dispersed (Lee, 2007; Jiang and Jin, 2017; Liu et al., 2017), and the classification and centralized assignment of cars loaded into different Ro-Ro ships can facilitate the yard management of Ro-Ro terminals (Cordeau et al., 2011). However, studies have not focused on a centralized car layout for the loading of cars into Ro-Ro ships. It is necessary to develop a new assignment rule to overcome the drawbacks of AR-CT, i.e., the scattered car layout and the insufficient utilization of storage resources.

# 3 Problem description

## 3.1 The storage location assignment problem (SLAP)

Figure 2 summarizes some optimization problems related to Ro-Ro transportation. Based on customer requirements, shipping companies schedule Ro-Ro ships and create their stowage plans. Terminal administrators plan the berthing positions and times at the quay for arriving Ro-Ro ships. Moreover, based on the data on commercial cars undergoing transshipment, one zone or adjacent zones are selected for storing the cars loaded into a Ro-Ro ship. The selection of the assigned zones is closely related to the berth plan of Ro-Ro ships. The refined management of parking locations focuses on the assignment of individual cars in the selected zones, with the aim of promoting the efficient management of yard resources and ensuring the orderly entrance operations of cars into the zone and the loading operations of cars into the Ro-Ro ship. For instance, the Shanghai Haitong Ro-Ro Terminal adopts AR-CT to realize the efficient management of yard resources. Notably, the refined management of yard resources still pertains to the planning level. In the operation phase, commercial cars will successively arrive at the yard and enter their assigned locations. It is possible that early or late arrival of cars will occur because of chance factors. Hence, the resource assignment plan in the planning phase must be rescheduled locally to handle unexpected events.

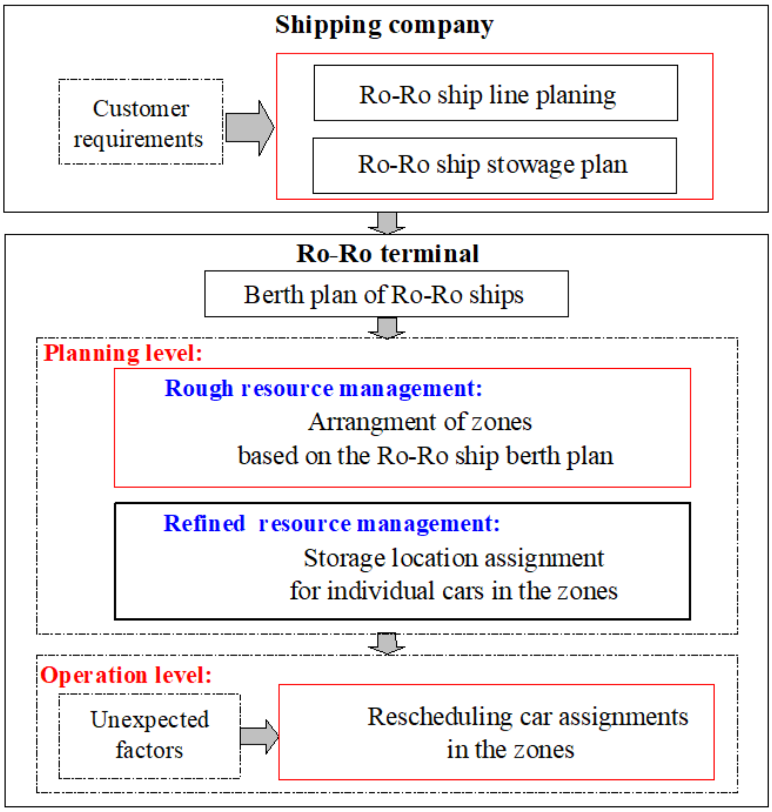


Figure 2 Optimization problems related to Ro-Ro transportation

In this paper, the SLAP involves assigning yard storage locations for arriving cars at one automotive Ro-Ro terminal, as depicted by the black frame in Figure 2. The SLAP is described as follows:

(a) Focusing on the storage location assignment of individual cars and the refined management of storage resources;

(b) Formulating a centralized car layout associated with the ship-loading sequences to improve ship-loading efficiency and the utilization of yard resources.

As shown in Figure 1, the loading areas contain many zones of different sizes that are used to store arriving cars for different ships. Cars that are to be loaded into the same ship should be assigned to one zone or adjacent zones as often as possible. However, the SLAP in this paper considers the assignment of individual cars in the designated zone/zones rather than the selection of the zone/zones, and it emphasizes the refined management of yard resources. Here, we assume that the size of the storage location is sufficient to store cars. The refined management of parking locations is still addressed at the planning level. Based on the order information provided by customers, port administrators assign the locations at which arriving cars will be stored over a planned period. Regarding the planning level, the car information is deterministic and known to port administrators.

In this paper, the SLAP emphasizes the development of a centralized car layout associated with the ship-loading sequence. The challenge is to ensure the feasibility of the routes of cars in the zones and to avoid the deadlock situation presented in Section 3.2.

### 3.2 Two deadlock situations in the SLAP

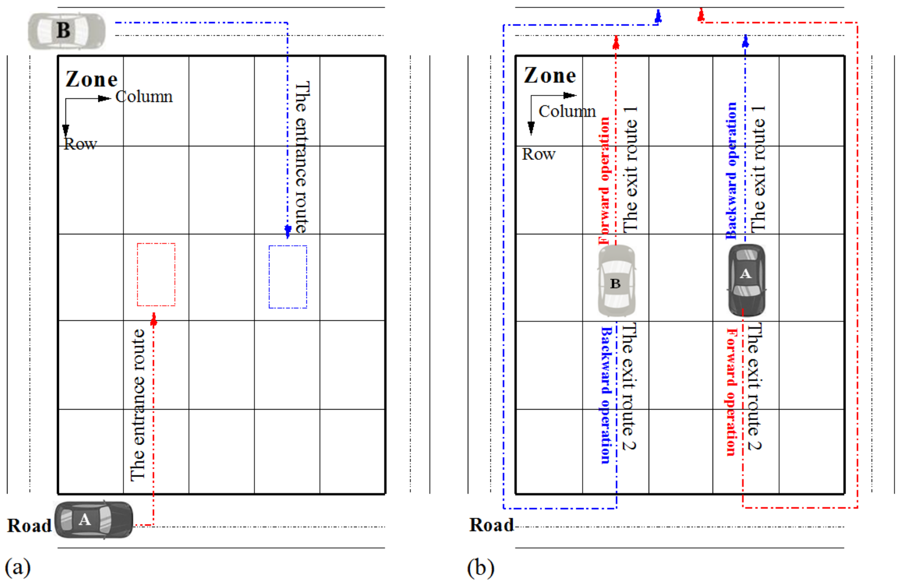


Figure 3 The feasible routes of cars in the zone: (a) entrance routes; and (b) exit routes

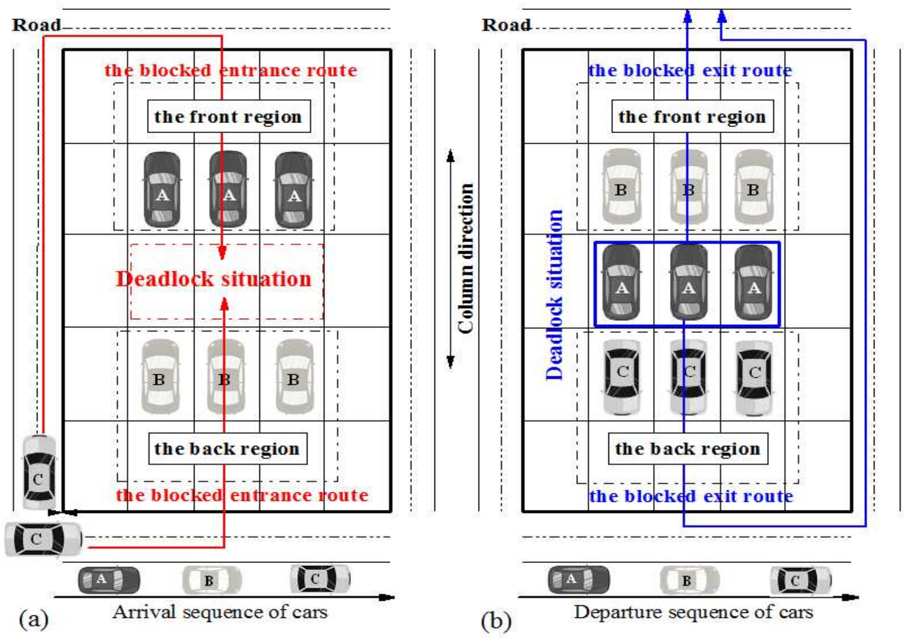


Figure 4 Two deadlock situations resulting from blocked routes: (a) blocked entrance routes; and (b) blocked exit routes

A feasible car assignment plan should ensure that arriving cars enter and exit the assigned storage location in the zone, and deadlock situations must be avoided. Here, a deadlock situation is one in which a car cannot be moved. To describe the coordinates of each storage location in the zone, we adopt rows and columns, and the car lengths are oriented in the column direction. Note that the backward operation of cars in the zone is allowed. For example, in Figure 3(b), cars A and B can exit from the zone along either route 1 or route 2.

The first deadlock situation represents an infeasible assignment resulting in blocked entrance routes. As shown in Figure 4(a), the entrance routes of type-C cars are blocked by type-A cars and type-B cars, and type-C cars cannot reach their appointed storage locations. Figure 4(b) presents another deadlock situation. In this situation, type-A cars cannot depart from the zone because their exit routes are blocked by type-B cars and type-C cars, which have later departure sequences.

Although relocation can resolve the deadlock situations, as presented in Section 2, it not only increases the risk of damage to cars but also causes traffic congestion at the port. Hence, feasible routes for cars entering or exiting their storage locations should be ensured.

## 3.3 An assignment rule based on car type (AR-CT)

- **The characteristics of AR-CT**

In AR-CT, all cars belonging to a type are the same. Cars of the same type are assigned in an orderly fashion to the zone along the column direction, and at most two types of cars are allowed to be stored in one column of a zone.

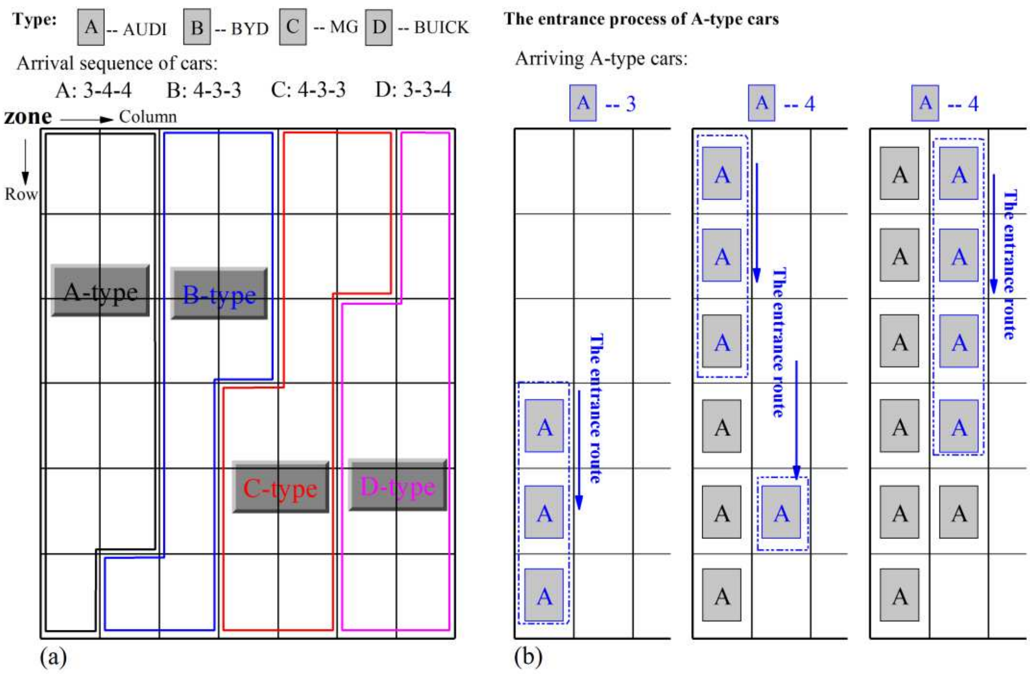


Figure 5 (a) The characteristics of AR-CT and (b) the entrance process of cars into a zone

Figure 5(a) presents a simple example to describe the characteristics of AR-CT, in which 42 cars loaded into a ship are assigned to one zone (6 rows and 7 columns). These cars are classified into four types based on brand differences. We adopt the letters A, B, C and D to indicate the types of cars. Importantly, all cars belonging to a type are considered to be the same. Every car type is matched with one region of the zone based on the number of cars, and at most, two car types are arranged in one column of the zone.

- **The feasible routes of cars in AR-CT**

As shown in Figure 5(b), although the arrival sequences of cars belonging to the same type are different, the feasible routes of cars entering the zone can be ensured because at most two types of cars are assigned to each column of one zone in AR-CT. For example, Figure 5(b) shows the entrance process of type-A cars in detail.

Usually, cars from different suppliers are first stored in the yard and then loaded into an arriving Ro-Ro ship (Jiang et al., 2014). Considering the differences in destinations, cars have predetermined loading regions in the Ro-Ro ship, i.e., the Ro-Ro ship stowage plan. As shown in Figure 6, 42 cars will be transported to three destinations (ship-unloading ports I, II, and III) and will correspondingly be loaded into three different regions of the Ro-Ro ship. Based on the Ro-Ro ship stowage plan, cars loaded into the same ship should satisfy the first-in-last-out loading rule. Therefore, cars in the zone will possess different ship-loading (departure) sequences to match their different ship-unloading sequences.

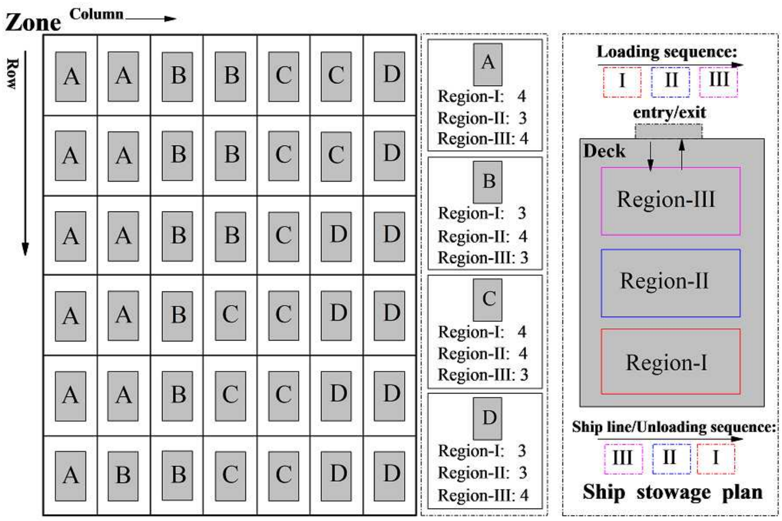


Figure 6 A car layout based on AR-CT and the ship stowage plan

Figure 6 presents the number of cars in each type loaded into three regions of a Ro-Ro ship. Although cars of the same type may be loaded into different regions of the Ro-Ro ship, it is unnecessary to identify the ID of each car in one type because all cars in one type are considered to be the same. Hence, the ship-loading process is as shown in Figure 7. Clearly, the feasible routes of cars exiting the yard can be ensured under different ship-loading sequences because cars of one type are the same and no more than two car types are assigned to each column of the zone.

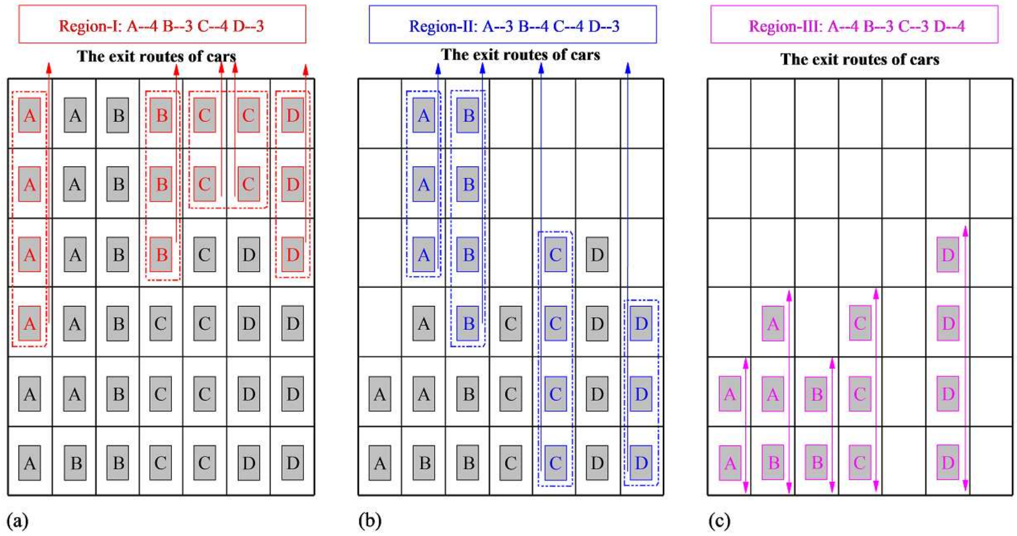

Figure 7 The loading process of cars from the zone to the Ro-Ro ship in AR-CT

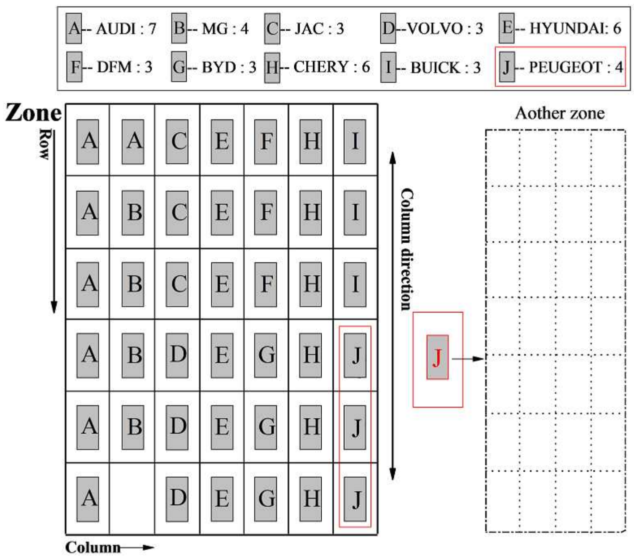

Figure 8 A simple example describing the insufficient use of storage resources in AR-CT

- **The drawbacks of AR-CT**

Although AR-CT ensures feasible routes for cars in the zone, cars with the same ship-loading sequence may be dispersed throughout the zone. For example, in Figure 7(a), the cars first loaded into region-I of the Ro-Ro ship are scattered throughout the zone, including four car types (A, B, C and D) indicated by the red frame. The same characteristic applies to the cars loaded into region-II and region-III of the Ro-Ro ship. Clearly, during the ship-loading process, the scattered layout of cars with the same departure sequence is not beneficial for the ship-loading operation. Figure 7 is a small example that describes the drawback of a practical assignment method based on AR-CT. For a large zone, this scattered car layout will result in a disorderly ship-loading process, uncoordinated operations among the drivers in a team, and increased time spent finding cars.

In addition to the influence on ship-loading efficiency, AR-CT is not beneficial for the use of storage resources, as it does not allow more than two types of cars to be arranged in the same column of a zone. Each type of car is differentiated based on version, brand and supplier, and one car brand may include dozens of types. Figure 8 shows an assignment result of 10 car types in a zone based on AR-CT, in which one type-J car must be assigned to another zone. This figure presents one possible case of the insufficient use of storage resources resulting from AR-CT. In a larger zone, the possibility of an insufficient use of storage resources increases with the increase in car types.

### 3.4 An assignment rule based on car group (AR-CG)

Considering the drawbacks of AR-CT, we present another assignment method. As shown in Figure 9, cars are assigned to a zone based on their loading regions in a Ro-Ro ship. Different from Figure 7, this car layout is advantageous for the intensive loading operation of cars with the same ship-loading sequence, and it helps improve ship-loading efficiency and reduce storage resource waste. Based on the car layout characteristics in Figure 9, the concept of a car group based on the Ro-Ro ship stowage plan is introduced. Moreover, a new assignment rule based on the car group (AR-CG) is presented.

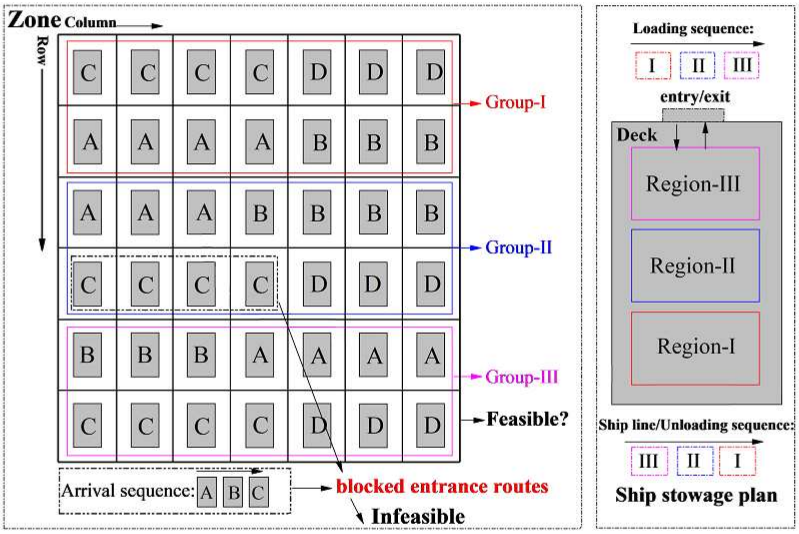


Figure 9 A car layout based on AR-CG

- **Car groups**

Groups have been widely applied to yard management at container and automotive Ro-Ro terminals (Nishimura et al., 2009; Woo and Kim, 2011; Jeong et al., 2012; Fischer and Gehring, 2005; Cordeau et al., 2011; Iannone et al. 2016). The car group presented in this paper is related to the Ro-Ro ship stowage plan. Cars loaded into the same region of a Ro-Ro ship constitute one car group. To distinguish the car group from the car type, we adopt Roman numerals to indicate the car groups (Figure 9); for example, all cars loaded into region-I of a Ro-Ro ship represent group-I.

The characteristics of car groups can be summarized as follows: (1) the arrival sequences of cars belonging to the same group may be different, and (2) different car groups have different ship-loading sequences depending on the Ro-Ro ship stowage plan. For example, in Figure 9, the cars belonging to group-I should first be loaded into region-I of the deck; consequently, they will be the last to be unloaded.

- **Dispersion degree**

As shown in Figure 9, cars belonging to a group are assigned to one zone. Here, we introduce a quantitative indicator called the dispersion degree to quantify the lack of compactness of the spatial layout of a single car group in the zone.

The dispersion degree is defined as the ratio of the rectangular region covered by cars to the number of cars. Assume that group-$g$ cars are assigned to the zone and that the number of cars is $n_g$. Binary variable $\varsigma_{g,([r_1,r_2],[c_1,c_2])}$ is adopted to identify whether all group-$g$ cars are assigned to the region framed by rows $[r_1,r_2]$ and columns $[c_1,c_2]$. The dispersion degree of group-$g$ cars can be expressed by Eq. (2).

$$\varsigma_{g,([r_1,r_2],[c_1,c_2])} = \begin{cases} 1 & \text{if all group-}g\text{ cars are assigned to the } ([\mathrm{r}_1,\mathrm{r}_2],[\mathrm{c}_1,\mathrm{c}_2]) \text{ region} \\ 0 & \text{otherwise} \end{cases} \tag{1}$$

$$f_g = \Big(\sum_{r_1 \in R} \sum_{c_1 \in C} \sum_{r_2 \in R | r_2 \geq r_1} \sum_{c_2 \in C | c_2 \geq c_1} (r_2 - r_1 + 1) \cdot (c_2 - c_1 + 1) \cdot \varsigma_{g,([r_1,r_2],[c_1,c_2])}\Big) / n_g \tag{2}$$

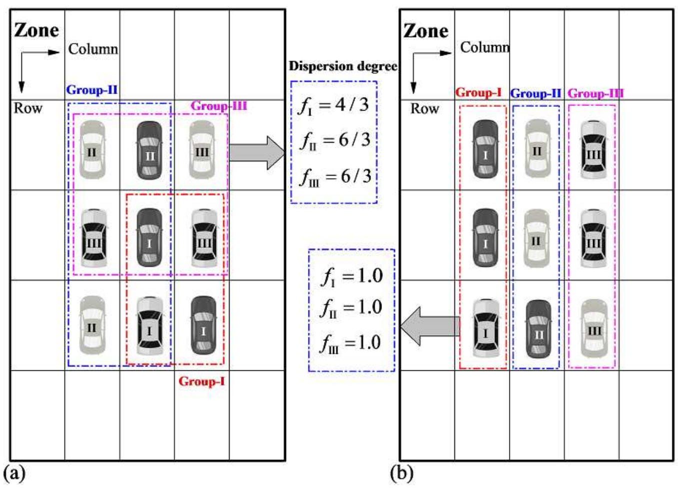


Figure 10 The dispersion degrees in two scenarios: (a) a scattered car layout and (b) a centralized car layout

Figure 10 gives two simple examples with scattered and centralized car layouts and illustrates the dispersion degree calculation in one zone. In the scattered car layout (Figure 10(a)), the dispersion degrees of the three car groups are 4/3, 2.0 and 2.0, and in the centralized car layout (Figure 10(b)), the dispersion degrees are 1.0, 1.0 and 1.0. Clearly, a smaller dispersion degree indicates a more centralized level of car assignment within the same group.

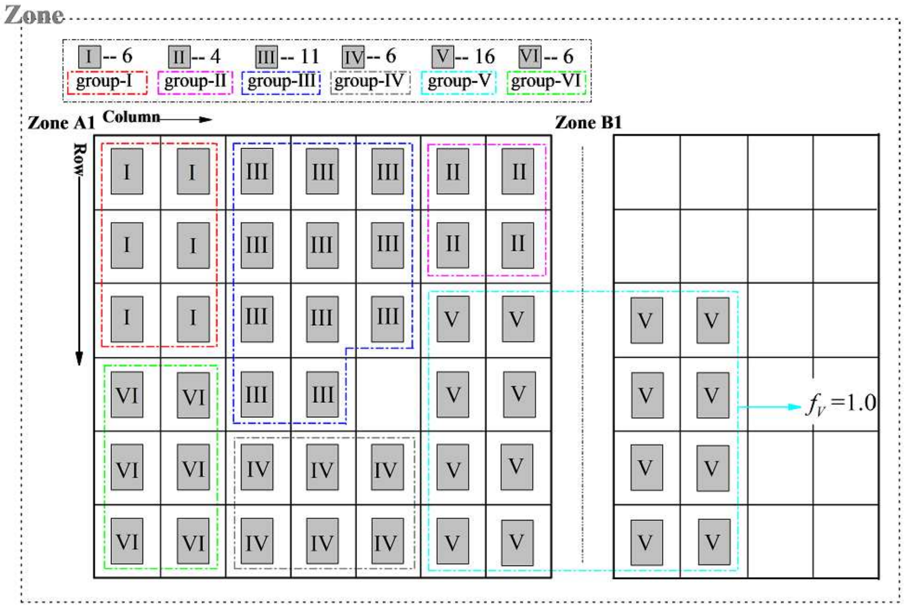


Figure 11 The dispersion degree in multiple zones

Figure 11 presents a small example of dispersion degree calculation in multiple zones. As shown in Figure 1, different zones are separated by the roadway, and commercial cars are not allowed to be parked along the roadway. Hence, the selected zones can be regarded as a large merged zone. The roadway inside the large zone is not considered to be space covered by the rectangular region. Arriving cars are assigned to two adjacent zones (A1 and B1). Although group-V cars are assigned simultaneously to zones A1 and B1, the group's dispersion degree is still 1.0. Hence, the dispersion degree calculation is not only suitable for the assignment of cars in one zone but also can be easily extended to multiple zones.

- **The major challenge of AR-CG**

As shown in Section 3.3, although route availability is guaranteed, the drawbacks of AR-CT are clear. We consider the application of AR-CG in the SLAP. However, in AR-CG, avoiding deadlock situations, in which a blocked entrance or exit route results in an infeasible car assignment in the zone, is a major challenge. For example, in Figure 9, based on the order information provided by customers, type-A cars arrive at the yard earlier than type-C cars; then, type-C cars cannot enter their appointed locations because of the blocked entrance route. Hence, a centralized car layout associated with the ship-loading sequence should ensure feasible routes for cars in the zone.

# 4 Mathematical formulation

## 4.1 Notations

Table 1: Symbols adopted in the model

| **Set and index** |
|---|

| | |
|---|---|
| $R$ | Set of rows in the zone, indexed by $r$, i.e., $R=\{1,2,...,r,...,\lvert \mathrm{R} \rvert\}$. |
| $C$ | Set of columns in the zone, indexed by $c$, i.e., $C=\{1,2,...,c,...,\lvert \mathrm{C} \rvert\}$. |
| $U$ | Set of arriving cars, indexed by $u$ or $v$, $U=\{1,2,...,u,...,v,...\lvert \mathrm{U} \rvert\}$. |
| $W$ | Set of existing cars, indexed by $w$, $W=\{1,2,...,w,...,\lvert \mathrm{W} \rvert\}$. |
| $G$ | Set of car groups, indexed by $g$, $G=\{1,2,...,g,...,\lvert \mathrm{G} \rvert\}$. |
| **Parameters** | |
| $t_u^a$ | Arrival time of car $u$ at the yard. |
| $t_u^d$ | Departure time of car $u$ from the yard. |
| $Y_w^{(r,c)}$ | Binary parameter: 1 if existing car $w$ is located in $(r,c)$; 0 otherwise. |
| $B_{g,u}$ | Binary parameter: 1 if car $u$ belongs to group-*g*; 0 otherwise. |
| $K_{u,v}$ | Binary parameter: 1 if $t_u^d > t_v^a$ and $t_u^a < t_v^d$; 0 otherwise. |
| $K_{u,w}$ | Binary parameter: 1 if $t_u^d > t_w^a$ and $t_u^a < t_w^d$; 0 otherwise. |
| $A_{u,v}$ | Binary parameter: 1 if $t_u^a < t_v^a$; 0 otherwise. |
| $A_{u,w}$ | Binary parameter: 1 if $t_u^a < t_w^a$; 0 otherwise. |
| $P_{u,v}$ | Binary parameter: 1 if $t_u^d < t_v^d$; 0 otherwise. |
| $P_{u,w}$ | Binary parameter: 1 if $t_u^d < t_w^d$; 0 otherwise. |
| **Variables** | |
| $x_u^{(r,c)}$ | Binary variable: 1 if car $u$ is assigned to location $(r,c)$; 0 otherwise. |
| $\mu_{u,(r,c)}^{I}$ | Binary variable: 1 if $x_u^{(r,c)}=1$ and a previous arriving car is assigned to the front region of location $(r,c)$; 0 otherwise. |
| $\mu_{u,(r,c)}^{II}$ | Binary variable: 1 if $x_u^{(r,c)}=1$ and a previous arriving car is assigned to the back region of location $(r,c)$; 0 otherwise. |
| $\lambda_{u,(r,c)}^{I}$ | Binary variable: 1 if $x_u^{(r,c)}=1$ and a later departing car is assigned to the front region of location $(r,c)$; 0 otherwise. |
| $\lambda_{u,(r,c)}^{II}$ | Binary variable: 1 if $x_u^{(r,c)}=1$ and a later departing car is assigned to the back region of location $(r,c)$; 0 otherwise. |
| $\xi_{g,r}$ | Auxiliary binary variable: 1 if group-*g* cars exist in row $r$; 0 otherwise. |
| $\zeta_{g,c}$ | Auxiliary binary variable: 1 if group-*g* cars exist in column $c$; 0 otherwise. |
| $\alpha_{g,r_1}^{R}$ | Auxiliary binary variable: 1 if the row lower border of the group-*g* car layout is $r_1$; 0 otherwise. |
| $\beta_{g,r_2}^{R}$ | Auxiliary binary variable: 1 if the row upper border of the group-*g* car layout is $r_2$; 0 otherwise. |
| $\alpha_{g,c_1}^{C}$ | Auxiliary binary variable: 1 if the column left border of the group-*g* car layout is $c_1$; 0 otherwise. |
| $\beta_{g,c_2}^{C}$ | Auxiliary binary variable: 1 if the column right border of the group-*g* car layout is $c_2$; 0 otherwise. |

| | |
|---|---|
| $\gamma^{R}_{g,[r_1,r_2]}$ | Auxiliary binary variable: 1 if rows $r_1$ and $r_2$ are, respectively, the lower and upper borders of the region that contains all group-$g$ cars; 0 otherwise. |
| $\gamma^{C}_{g,[c_1,c_2]}$ | Auxiliary binary variable: 1 if columns $c_1$ and $c_2$ are, respectively, the left and right borders of the region that contains all group-$g$ cars; 0 otherwise. |
| $\varsigma_{g,([r_1,r_2],[c_1,c_2])}$ | Auxiliary binary variable: 1 if $([r_1,r_2],[c_1,c_2])$ is the smallest rectangular region that contains all group-$g$ cars; 0 otherwise. |

## 4.2 Model

$$\min f = \sum_{g\in G}\left(\frac{\sum_{r_1\in R}\sum_{c_1\in C}\sum_{r_2\in R|r_2\geq r_1}\sum_{c_2\in C|c_2\geq c_1}(r_2-r_1+1)\cdot(c_2-c_1+1)\cdot\varsigma_{g,([r_1,r_2],[c_1,c_2])}}{\sum_{u\in U}B_{g,u}+\sum_{w\in W}B_{g,w}}\right) \tag{3}$$

Subject to:

**(I) Storage location constraints:**

$$\sum_{r\in R}\sum_{c\in C}x_u^{(r,c)}=1 \qquad \forall\, u\in U \tag{4}$$

$$x_u^{(r,c)}+x_v^{(r,c)}\leq 2-K_{u,v} \qquad \forall\, u,v\in U, u\neq v;\ r\in R;\ c\in C \tag{5a}$$

$$x_u^{(r,c)}+Y_w^{(r,c)}\leq 2-K_{u,w} \qquad \forall\, u\in U;\ w\in W;\ r\in R;\ c\in C \tag{5b}$$

**(II) Deadlock avoidance constraints:**

$$\mu^{I}_{u,(r,c)}\leq\sum_{r'=1}^{r-1}\Big(\sum_{v\in U|v\neq u}x_v^{(r',c)}\cdot K_{u,v}\cdot A_{u,v}+\sum_{w\in W}Y_w^{(r',c)}\cdot K_{u,w}\cdot A_{u,w}\Big)$$

$$\forall\, u\in U;\ r\in R, r>1;\ c\in C \tag{6a}$$

$$x_u^{(r,c)}\geq\mu^{I}_{u,(r,c)} \qquad \forall\, u\in U;\ r\in R, r>1;\ c\in C \tag{6b}$$

$$x_u^{(r,c)}\leq\mu^{I}_{u,(r,c)}+(1-x_v^{(r',c)}\cdot K_{u,v}\cdot A_{u,v})$$

$$\forall\, u\in U;\ v\in U, v\neq u;\ r\in R, r>1;\ r'\in R, 1\leq r'<r;\ c\in C \tag{6c}$$

$$x_u^{(r,c)}\leq\mu^{I}_{u,(r,c)}+(1-Y_w^{(r',c)}\cdot K_{u,w}\cdot A_{u,w})$$

$$\forall\, u\in U;\ w\in W;\ r\in R, r>1;\ r'\in R, 1\leq r'<r;\ c\in C \tag{6d}$$

$$\mu^{I}_{u,(r,c)}=0 \qquad \forall\, u\in U;\ r=1;\ c\in C \tag{6e}$$

$$\mu^{II}_{u,(r,c)}\leq\sum_{r'=r+1}^{|R|}\Big(\sum_{v\in U|v\neq u}x_v^{(r',c)}\cdot K_{u,v}\cdot A_{u,v}+\sum_{w\in W}Y_w^{(r',c)}\cdot K_{u,w}\cdot A_{u,w}\Big)$$

$$\forall\ u \in U;\ r \in R, r < |\mathrm{R}|;\ c \in C \qquad (7a)$$

$$x_u^{(r,c)} \geq \mu_{u,(r,c)}^{II} \qquad \forall\ u \in U;\ r \in R, r < |\mathrm{R}|;\ c \in C \qquad (7b)$$

$$x_u^{(r,c)} \leq \mu_{u,(r,c)}^{II} + (1 - x_v^{(r',c)} \cdot K_{u,v} \cdot A_{u,v})$$

$$\forall\ u, v \in U, u \neq v;\ r \in R, r < |\mathrm{R}|;\ r' \in R, r < r' \leq |\mathrm{R}|;\ c \in C \qquad (7c)$$

$$x_u^{(r,c)} \leq \mu_{u,(r,c)}^{II} + (1 - Y_w^{(r',c)} \cdot K_{u,w} \cdot A_{u,w})$$

$$\forall\ u \in U;\ w \in W;\ r \in R, r < |\mathrm{R}|;\ r' \in R, r < r' \leq |\mathrm{R}|;\ c \in C \qquad (7d)$$

$$\mu_{u,(r,c)}^{II} = 0 \qquad \forall\ u \in U;\ r = |\mathrm{R}|;\ c \in C \qquad (7e)$$

$$x_u^{(r,c)} + \mu_{u,(r,c)}^{I} + \mu_{u,(r,c)}^{II} \leq 2 \qquad \forall\ u \in U;\ r \in R;\ c \in C \qquad (8)$$

$$\lambda_{u,(r,c)}^{I} \leq \sum_{r'=1}^{r-1} \Big( \sum_{v \in U | v \neq u} x_v^{(r',c)} \cdot K_{u,v} \cdot P_{u,v} + \sum_{w \in W} Y_w^{(r',c)} \cdot K_{u,w} \cdot P_{u,w} \Big)$$

$$\forall\ u \in U;\ r \in R, r > 1;\ c \in C \qquad (9a)$$

$$x_u^{(r,c)} \geq \lambda_{u,(r,c)}^{I} \qquad \forall\ u \in U;\ r \in R, r > 1;\ c \in C \qquad (9b)$$

$$x_u^{(r,c)} \leq \lambda_{u,(r,c)}^{I} + (1 - x_v^{(r',c)} \cdot K_{u,v} \cdot P_{u,v})$$

$$\forall\ u, v \in U, u \neq v;\ r \in R, r > 1;\ r' \in R, 1 \leq r' < r;\ c \in C \qquad (9c)$$

$$x_u^{(r,c)} \leq \lambda_{u,(r,c)}^{I} + (1 - Y_w^{(r',c)} \cdot K_{u,w} \cdot P_{u,w})$$

$$\forall\ u \in U;\ w \in W;\ r \in R, r > 1;\ r' \in R, 1 \leq r' < r;\ c \in C \qquad (9d)$$

$$\lambda_{u,(r,c)}^{I} = 0 \qquad \forall\ u \in U;\ r = 1;\ c \in C \qquad (9e)$$

$$\lambda_{u,(r,c)}^{II} \leq \sum_{r'=r+1}^{|\mathrm{R}|} \Big( \sum_{v \in U | v \neq u} x_v^{(r',c)} \cdot K_{u,v} \cdot P_{u,v} + \sum_{w \in W} Y_w^{(r',c)} \cdot K_{u,w} \cdot P_{u,w} \Big)$$

$$\forall\ u \in U;\ r \in R, r < |\mathrm{R}|;\ c \in C \qquad (10a)$$

$$x_u^{(r,c)} \geq \lambda_{u,(r,c)}^{II} \qquad \forall\ u \in U;\ r \in R, r < |\mathrm{R}|;\ c \in C \qquad (10b)$$

$$x_u^{(r,c)} \leq \lambda_{u,(r,c)}^{II} + (1 - x_v^{(r',c)} \cdot K_{u,v} \cdot P_{u,v})$$

$$\forall\ u, v \in U, u \neq v;\ r \in R, r < |\mathrm{R}|;\ r' \in R, r < r' \leq |\mathrm{R}|;\ c \in C \qquad (10c)$$

$$x_u^{(r,c)} \leq \lambda_{u,(r,c)}^{II} + (1 - Y_w^{(r',c)} \cdot K_{u,w} \cdot P_{u,w})$$

$$\forall\ u\in U;\ w\in W;\ r\in R, r<|\mathrm{R}|;\ r^{'}\in R, r<r^{'}\le|\mathrm{R}|;\ c\in C \tag{10d}$$

$$\lambda^{II}_{u,(r,c)}=0 \qquad \forall\ u\in U;\ r=|\mathrm{R}|;\ c\in C \tag{10e}$$

$$x_u^{(r,c)}+\lambda^{I}_{u,(r,c)}+\lambda^{II}_{u,(r,c)}\le 2 \qquad \forall\ u\in U;\ r\in R;\ c\in C \tag{11}$$

**(III) Car layout identification:**

$$\xi_{g,r}\cdot|\mathrm{C}|\ge\sum_{c\in C}\Big(\sum_{u\in U}x_u^{(r,c)}\cdot B_{g,u}+\sum_{w\in W}Y_w^{(r,c)}\cdot B_{g,w}\Big) \qquad \forall\ g\in G;\ r\in R \tag{12a}$$

$$\zeta_{g,c}\cdot|\mathrm{R}|\ge\sum_{r\in R}\Big(\sum_{u\in U}x_u^{(r,c)}\cdot B_{g,u}+\sum_{w\in W}Y_w^{(r,c)}\cdot B_{g,w}\Big) \qquad \forall\ g\in G;\ c\in C \tag{12b}$$

$$\sum_{r\in R}\left(\alpha^{R}_{g,r}\cdot r\right)\ge\xi_{g,r_1}\cdot r_1 \qquad \forall\ g\in G;\ r\in R \tag{13a}$$

$$\sum_{r\in R}\alpha^{R}_{g,r}\le 1 \qquad \forall\ g\in G \tag{13b}$$

$$\sum_{r\in R}\left(\beta^{R}_{g,r}\cdot r\right)\le\xi_{g,r_2}\cdot r_2+|\mathrm{R}|\cdot\left(1-\xi_{g,r_2}\right) \qquad \forall\ g\in G;\ r_2\in R \tag{14a}$$

$$\sum_{r\in R}\beta^{R}_{g,r}\le 1 \qquad \forall\ g\in G \tag{14b}$$

$$\sum_{c\in C}\left(\alpha^{C}_{g,c}\cdot c\right)\ge\zeta_{g,c_1}\cdot c_1 \qquad \forall\ g\in G;\ c_1\in C \tag{15a}$$

$$\sum_{c\in C}\alpha^{C}_{g,c}\le 1 \qquad \forall\ g\in G \tag{15b}$$

$$\sum_{c\in C}\left(\beta^{C}_{g,c}\cdot c\right)\le\zeta_{g,c_2}\cdot c_2+|\mathrm{C}|\cdot\left(1-\zeta_{g,c_2}\right) \qquad \forall\ g\in G;\ c_2\in C \tag{16a}$$

$$\sum_{c\in C}\beta^{C}_{g,c}\le 1 \qquad \forall\ g\in G \tag{16b}$$

$$\gamma^{R}_{g,[r_1,r_2]}\ge\alpha^{R}_{g,r_1}+\beta^{R}_{g,r_2}-1 \qquad \forall\ g\in G;\ r_1,r_2\in R, r_1\le r_2 \tag{17a}$$

$$\gamma^{R}_{g,[r_1,r_2]}\cdot 2\le\alpha^{R}_{g,r_1}+\beta^{R}_{g,r_2} \qquad \forall\ g\in G;\ r_1,r_2\in R, r_1\le r_2 \tag{17b}$$

$$\gamma^{C}_{g,[c_1,c_2]}\ge\alpha^{C}_{g,c_1}+\beta^{C}_{g,c_2}-1 \qquad \forall\ g\in G;\ c_1,c_2\in C, c_1\le c_2 \tag{18a}$$

$$\gamma^{C}_{g,[c_1,c_2]}\cdot 2\le\alpha^{C}_{g,c_1}+\beta^{C}_{g,c_2} \qquad \forall\ g\in G;\ c_1,c_2\in C, c_1\le c_2 \tag{18b}$$

$$\varsigma_{g,([r_1,r_2],[c_1,c_2])}\ge\gamma^{R}_{g,[r_1,r_2]}+\gamma^{C}_{g,[c_1,c_2]}-1 \qquad \forall\ g\in G;\ r_1,r_2\in R, r_1\le r_2;\ c_1,c_2\in C, c_1\le c_2 \tag{19a}$$

$$\varsigma_{g,([r_1,r_2],[c_1,c_2])}\cdot 2\le\gamma^{R}_{g,[r_1,r_2]}+\gamma^{C}_{g,[c_1,c_2]} \qquad \forall\ g\in G;\ r_1,r_2\in R, r_1\le r_2;\ c_1,c_2\in C, c_1\le c_2 \tag{19b}$$

**(IV) 0-1 variables:**

$$x_u^{(r,c)},\lambda^{I}_{u,(r,c)},\lambda^{II}_{u,(r,c)},\mu^{I}_{u,(r,c)},\mu^{II}_{u,(r,c)}\in\{0,1\} \qquad \forall\ u\in U;\ r\in R;\ c\in C \tag{20a}$$

$$\xi_{g,r}, \zeta_{g,c}, \alpha^R_{g,r}, \beta^R_{g,r}, \alpha^C_{g,c}, \beta^C_{g,c} \in \{0,1\} \qquad \forall\ g \in G;\ r \in R;\ c \in C \tag{20b}$$

$$\gamma^R_{g,[r_1,r_2]}, \gamma^C_{g,[c_1,c_2]}, \varsigma_{g,([r_1,r_2],[c_1,c_2])} \in \{0,1\} \qquad \forall\ g \in G;\ r_1,r_2 \in R, r_1 \le r_2;\ c_1,c_2 \in C, c_1 \le c_2 \tag{20c}$$

We formulate the SLAP as a linear 0-1 integer programming model that attempts to minimize the total dispersion degrees of all car groups in the zone during the planned time period $[T_1, T_s]$. The model assigns the location of every car in the zone, as indicated by binary variable $x_u^{(r,c)}$. The set of arriving cars is indicated by $U = \{1,...,u,...,|U|\}$, and car groups are denoted by $G = \{1,...,g,...,|G|\}$. If a certain location is occupied before planned time $T_1$, then it cannot be assigned to an arriving car until the existing car departs from the yard. The set of existing cars is indicated by $W = \{1,...,w,...,|W|\}$, and binary parameter $Y_w^{(r,c)}$ is adopted to indicate the locations occupied by existing cars in the zone.

Each car in sets $U$ and $W$ is identified by three parameters: arrival time $t_u^a$, departure time $t_u^d$, and group character $B_{g,u}$. Note that the value of $B_{g,u}$ can be easily identified based on the Ro-Ro ship stowage plan and the information of arrival cars. The rows and columns of the zone are indicated by sets $R = \{1,...,r,...,|R|\}$ and $C = \{1,...,c,...,|C|\}$, respectively.

- **Storage location constraints**

Constraint (4) ensures that a car is assigned to only one location in the zone, while constraint (5a) guarantees that each location in the zone is occupied by at most one car at a time. Because a storage location is released when a car departs from the zone, another arriving car can be assigned to the location. Therefore, binary parameter $K_{u,v}$ is used to identify whether the storage times of two cars intersect, i.e., if $t_u^d > t_v^a$ and $t_u^a < t_v^d$, then $K_{u,v} = 1$; otherwise, $K_{u,v} = 0$. If $K_{u,v} = 0$, then constraint (5a) is redundant, which means cars $u$ and $v$ can be assigned to the same location in the zone. Clearly, the proposed model is compatible with the case in which the cars loaded into different ships share a zone. Constraint (5b) emphasizes that locations occupied by existing cars cannot be assigned to arriving cars until these existing cars depart from the yard.

- **Deadlock avoidance constraints**

Constraints (6)-(11) prevent the two deadlock situations presented in Section 3.2. Constraints (6)-(8) ensure the availability of entrance routes. First, binary parameter $A_{u,v}$ is used to describe the arrival order of cars $u$ and $v$. Then, binary variable $\mu^I_{u,(r,c)}$ is introduced to identify whether a blocked entrance route is formed in the front region of location $(r,c)$ if car $u$ is assigned to location $(r,c)$. The definition is presented in Eq. (21a).

$$\mu^{I}_{u,(r,c)} = \begin{cases} 1 & \text{if } x_u^{(r,c)} = 1, \text{ and } r > 1, \text{ and } \exists\, r^{'} (1 \le r^{'} < r), \\ & \exists\, v \in U,\ v \ne u \text{ and } x_v^{(r^{'},c)} \cdot K_{u,v} \cdot A_{u,v} = 1; \text{ or } \exists\, w \in W \text{ and } Y_w^{(r^{'},c)} \cdot K_{u,w} \cdot A_{u,w} = 1 \\ 0 & \text{if } x_u^{(r,c)} = 1, \text{ and } r = 1 \\ 0 & \text{othewise} \end{cases} \tag{21a}$$

$$\mu^{II}_{u,(r,c)} = \begin{cases} 1 & \text{if } x_u^{(r,c)} = 1, \text{ and } r < |\mathrm{R}|, \text{ and } \exists\, r^{'} (r < r^{'} \le |\mathrm{R}|), \\ & \exists\, v \in U,\ v \ne u \text{ and } x_v^{(r^{'},c)} \cdot K_{u,v} \cdot A_{u,v} = 1; \text{ or } \exists\, w \in W \text{ and } Y_w^{(r^{'},c)} \cdot K_{u,w} \cdot A_{u,w} = 1 \\ 0 & \text{if } x_u^{(r,c)} = 1, \text{ and } r = |\mathrm{R}| \\ 0 & \text{othewise} \end{cases} \tag{21b}$$

The definition of binary variable $\mu^{I}_{u,(r,c)}$ shows that if $x_v^{(r^{'},c)} \cdot K_{u,v} \cdot A_{u,v} = 1$ ($\exists\, r^{'} : 1 \le r^{'} < r$), then early arriving car $v$ occupies the front region of location $(r,c)$ and blocks the front entrance route of car $u$ to the appointed location ($x_u^{(r,c)} = 1$); therefore, the value of $\mu^{I}_{u,(r,c)}$ is 1. The definition of $\mu^{I}_{u,(r,c)}$ also focuses on the influence of existing cars on the front entrance route of car $u$ to location $(r,c)$, i.e., if $Y_w^{(r^{'},c)} \cdot K_{u,w} \cdot A_{u,w} = 1$ ($\exists\, r^{'} : 1 \le r^{'} < r;\ w \in W$), then existing car $w$ blocks the front entrance route. If car $u$ is assigned to the border location ($r = 1$), then car $u$ can always enter the appointed location $\{(1,c) \mid c \in C\}$ without any blocking. Hence, the value of $\mu^{I}_{u,(r,c)}$ is always 0.

Constraint (6) presents the relationships among $\mu^{I}_{u,(r,c)}$, $x_u^{(r,c)}$ and $x_v^{(r^{'},c)}$. Constraint (6a) focuses on the scenario without a blocked front entrance route. If $\sum_{r^{'}=1}^{r-1} \left( \sum_{v \in U | v \ne u} x_v^{(r^{'},c)} \cdot K_{u,v} \cdot A_{u,v} + \sum_{w \in W} Y_w^{(r^{'},c)} \cdot K_{u,w} \cdot A_{u,w} \right) = 0$, then the value of $\mu^{I}_{u,(r,c)}$ is always zero, regardless of whether the value of $x_u^{(r,c)}$ is 1 or 0. If $\sum_{r^{'}=1}^{r-1} \left( \sum_{v \in U | v \ne u} x_v^{(r^{'},c)} \cdot K_{u,v} \cdot A_{u,v} + \sum_{w \in W} Y_w^{(r^{'},c)} \cdot K_{u,w} \cdot A_{u,w} \right) > 0$, then constraint (6a) is redundant. Constraints (6b)-(6d) apply to the case with a blocked entrance route. If early arriving car $v$ or existing car $w$ occupies the front region of location $(r,c)$, i.e., $x_v^{(r^{'},c)} \cdot K_{u,v} \cdot A_{u,v} = 1$ ($\forall\, v \in U, v \ne u;\ r^{'} \in R, 1 \le r^{'} < r$) or $Y_w^{(r^{'},c)} \cdot K_{u,w} \cdot A_{u,w} = 1$ ($\forall\, w \in W;\ r^{'} \in R, 1 \le r^{'} < r$), then constraints (6b, 6c) and (6b, 6d) become $x_u^{(r,c)} \ge \mu^{I}_{u,(r,c)}$ and $\mu^{I}_{u,(r,c)} \ge x_u^{(r,c)}$, respectively. Clearly, the value of $\mu^{I}_{u,(r,c)}$ depends on that of $x_u^{(r,c)}$, i.e., if $x_u^{(r,c)} = 1$, then $\mu^{I}_{u,(r,c)} = 1$; and if $x_u^{(r,c)} = 0$, then $\mu^{I}_{u,(r,c)} = 0$. Therefore, if car $u$ is assigned to location $(r,c)$ ($x_u^{(r,c)} = 1$), then it cannot enter the assigned position via the front route. Constraint (6e) represents the border condition, i.e., if car $u$ is assigned to a border location of the zone ( $r=1$ ), then the value of $\mu^{I}_{u,(r,c)}$ is always 0.

Similarly, binary variable $\mu^{II}_{u,(r,c)}$ is introduced to identify whether the back region of location $(r,c)$ is blocked by early arriving cars or existing cars, and its definition is presented in Eq. (21b). Constraints (7a)-(7e) focus on the development of the blocked entrance route in the back region of location $(r,c)$. Based on the identification of $\mu^{I}_{u,(r,c)}$ and $\mu^{II}_{u,(r,c)}$, constraint (8) ensures that if car $u$ is assigned to location $(r,c)$, then at least one entrance route for car $u$ is feasible; hence, the first deadlock situation is avoided.

Constraints (9)-(11) focus on the available exit routes of cars from the zone and avoid the occurrence of the second deadlock situation shown in Figure 4(b). The 0-1 parameter $P_{u,v}$ is introduced to describe the departure sequence of cars $u$ and $v$, i.e., if $t^{d}_{u}<t^{d}_{v}$, then $P_{u,v}=1$; otherwise, $P_{u,v}=0$. Similarly, binary variables $\lambda^{I}_{u,(r,c)}$ and $\lambda^{II}_{u,(r,c)}$ are introduced to identify blocked exit routes.

$$\lambda^{I}_{u,(r,c)}=\begin{cases}1 & \text{if } x^{(r,c)}_{u}=1, \text{ and } r>1, \text{ and } \exists\, r^{'}(1\le r^{'}<r), \\ & \exists\, v\in U,\ v\ne u \text{ and } x^{(r^{'},c)}_{v}\cdot K_{u,v}\cdot P_{u,v}=1; \text{ or } \exists\, w\in W \text{ and } Y^{(r^{'},c)}_{w}\cdot K_{u,w}\cdot P_{u,w}=1 \\ 0 & \text{if } x^{(r,c)}_{u}=1, \text{ and } r=1 \\ 0 & \text{othewise}\end{cases} \tag{22a}$$

$$\lambda^{II}_{u,(r,c)}=\begin{cases}1 & \text{if } x^{(r,c)}_{u}=1, \text{ and } r<|\mathrm{R}|, \text{ and } \exists\, r^{'}(r<r^{'}\le|\mathrm{R}|), \\ & \exists\, v\in U,\ v\ne u \text{ and } x^{(r^{'},c)}_{v}\cdot K_{u,v}\cdot P_{u,v}=1; \text{ or } \exists\, w\in W \text{ and } Y^{(r^{'},c)}_{w}\cdot K_{u,w}\cdot P_{u,w}=1 \\ 0 & \text{if } x^{(r,c)}_{u}=1, \text{ and } r=|\mathrm{R}| \\ 0 & \text{othewise}\end{cases} \tag{22b}$$

- **Car layout identification**

The dispersion degree of a car group depends on the identification of the layout region of the car group in the zone, i.e., the value of binary variable $\varsigma_{g,([r_1,r_2],[c_1,c_2])}$ in Eq. (2). The relationship between auxiliary variable $\varsigma_{g,([r_1,r_2],[c_1,c_2])}$ and decision variable $x^{(r,c)}_{u}$ must be determined. First, two auxiliary binary variables ( $\xi_{g,r}$ and $\zeta_{g,c}$ ) are defined to identify whether group-*g* cars are assigned to row $r$ and column $c$ in the zone, respectively. Then, constraints (12a) and (12b) represent the relationships among $\xi_{g,r}$, $\zeta_{g,c}$ and decision $x^{(r,c)}_{u}$, i.e., if $x^{(r,c)}_{u}=1$ and $B_{g,u}=1$, then $\xi_{g,r}=1$ and $\zeta_{g,c}=1$, respectively. Notably, the group characteristics of the existing cars are considered in constraints (12a) and (12b).

Second, based on the values of $\xi_{g,r}$ and $\zeta_{g,c}$, the four borders of the group-*g* car layout in the zone, i.e., the lower and upper borders of the rows and the right and left borders of the columns, are identified by four auxiliary binary variables: $\alpha^{R}_{g,r_1}$, $\beta^{R}_{g,r_2}$, $\alpha^{C}_{g,c_1}$, and $\beta^{C}_{g,c_2}$. Constraints (13a) and (14a) traverse each row in the zone from the lower to the upper borders of the rows covered by group-$g$ cars. Constraints (13b) and (14b) ensure the uniqueness of the lower and upper borders. Similarly, constraints (15) and (16) focus on the left and right borders of the columns covered by group-$g$ cars.

Moreover, we adopt auxiliary binary variable $\gamma^{R}_{g,[r_1,r_2]}$ to integrate the lower and upper borders of the rows covered by group-$g$ cars. Constraints (17a) and (17b) represent the relationships among $\alpha^{R}_{g,r_1}$, $\beta^{R}_{g,r_2}$ and $\gamma^{R}_{g,[r_1,r_2]}$, i.e., if and only if $\alpha^{R}_{g,r_1}=1$ and $\beta^{R}_{g,r_2}=1$, then $\gamma^{R}_{g,[r_1,r_2]}=1$. Similarly, the auxiliary binary variable $\gamma^{R}_{g,[r_1,r_2]}$ in constraints (18a) and (18b) integrates the left and right borders, respectively, of the columns covered by group-$g$ cars.

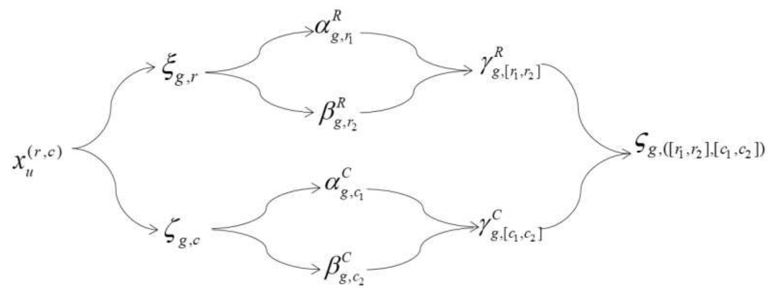


Figure 12 The logical relationship between $x_u^{(r,c)}$ and $\varsigma_{g,([r_1,r_2],[c_1,c_2])}$

Finally, constraints (19a) and (19b) identify the rectangular region covered by group-$g$ cars and determine the value of binary variable $\varsigma_{g,([r_1,r_2],[c_1,c_2])}$ based on $\gamma^{R}_{g,[r_1,r_2]}$ and $\gamma^{C}_{g,[c_1,c_2]}$, respectively. Notably, the definitions of the above auxiliary binary variables such as $\xi_{g,r}$, $\zeta_{g,c}$, $\alpha^{R}_{g,r_1}$, $\beta^{R}_{g,r_2}$, $\alpha^{C}_{g,c_1}$, $\beta^{C}_{g,c_2}$, $\gamma^{R}_{g,[r_1,r_2]}$ and $\gamma^{C}_{g,[c_1,c_2]}$ provide the relationship between decision variable $x_u^{(r,c)}$ and binary variable $\varsigma_{g,([r_1,r_2],[c_1,c_2])}$, and Figure 12 presents their logical relationship.

The proposed model is a linear 0-1 integer programming model that includes a large number of binary decision and auxiliary variables. It can be easily found that the binary variables related to car and location ( $x_u^{(r,c)}$ , $\mu^{I}_{u,(r,c)}$ , $\mu^{II}_{u,(r,c)}$ , $\lambda^{I}_{u,(r,c)}$ and $\lambda^{II}_{u,(r,c)}$ ) number approximately $5\cdot|\mathrm{U}|\cdot|\mathrm{R}|\cdot|\mathrm{C}|$ and that the binary variables related to car group ( $\xi_{g,r}$ , $\zeta_{g,c}$ , $\alpha^{R}_{g,r_1}$ , $\beta^{R}_{g,r_2}$ , $\alpha^{C}_{g,c_1}$ , $\beta^{C}_{g,c_2}$ , $\gamma^{R}_{g,[r_1,r_2]}$ and $\gamma^{C}_{g,[c_1,c_2]}$ ) number approximately $3\cdot|\mathrm{G}|\cdot|\mathrm{R}|+3\cdot|\mathrm{G}|\cdot|\mathrm{C}|+|G|\cdot|\mathrm{R}|^2+|G|\cdot|\mathrm{C}|^2$. Usually, the number of car groups is far smaller than that of car types, i.e., $\mathrm{G}| \ll |\mathrm{U}|$. Hence, the crucial factors influencing the complexity of the model are still the number of assigned cars and the scale of the selected zone.

Clearly, the complexity of the model is reduced if the route constraints are relaxed. A relaxed model with less complexity can be transformed into a typical graph coloring problem (GCP). Each location in the zone may be regarded as a node in an undirected graph. Moreover, each node can be graphed by one of K colors, which is equivalent to the number of car groups. The link rules between nodes are summarized as follows: (1) only adjacent nodes are allowed to link, and (2) two nodes with different colors can be linked. The object of a GCP is to minimize the number of links in the undirected graph. An optimal solution for this relaxed SLAP could be polynomially transformed into an optimal solution for the GCP. Therefore, if there is a pseudo-polynomial algorithm for the relaxed SLAP, then this algorithm will solve the GCP as well. However, it is well known that the GCP is a famous NP-hard problem. Hence, an efficient heuristic algorithm is necessary to obtain a satisfactory car layout within a finite computational time.

Based on constraint (5), if the value of parameter $K_{u,v}$ is zero, then two cars ($u$ and $v$) are allowed to be assigned to the same location in the zone because of the free conflict between the two cars. Therefore, a rolling-horizon approach based on closed-loop feedback, which will be illustrated in detail in Section 6, is designed to identify conflicts among cars and reduce the scale of the problem. Each phase in the rolling-horizon approach focuses on assigning cars with conflicts in the zone, i.e., $K_{u,v}=1$ [1]. The centralized car layout in the single phase is key to the efficiency of the rolling-horizon approach during the period. In Section 5, we present an HTSES for obtaining a centralized layout of cars with conflicts.

# 5 A hierarchical two-stage exchange strategy (HTSES)

## 5.1 The HTSES framework

An initial car layout is easily formulated by assigning arriving cars to the idle locations in the zone/zones. However, this assignment plan may be infeasible because of blocked car routes. Moreover, the car layout may greatly deviate from a centralized layout with minimal dispersion. Exchanges between cars and car movements can be used to develop a centralized car layout. For example, the scattered layout of cars in Figure 13(a) is modified to form a centralized layout via two car movements (Figure 13(c)), and the value of the dispersion degree is varied from 2.4 to 1.0.

However, the dispersion degree focuses on a static car layout in the zone, while the transformation of the car layout is a dynamic process of transition from a scattered layout to a centralized layout. The dispersion degree may be worse during car exchange and movement. As shown in Figure 13(a), the dispersion degree of group-I cars is approximately 2.4 in the initial car layout. The first movement in Figure 13(a) results in an increase in the dispersion degree ($f_I=3.0$), while the second movement produces a centralized car layout with minimal dispersion (Figure 13(c)). Clearly, considering only the dispersion degree may be insufficient for identifying the efficient exchanges or movements of cars to obtain a centralized layout with the minimum dispersion degree.

---

[1] For $K_{u,v}=1$ ($\forall u,v\in U$), constraint (5) is reduced to $x_u^{(r,c)}+x_v^{(r,c)}\le 1$.

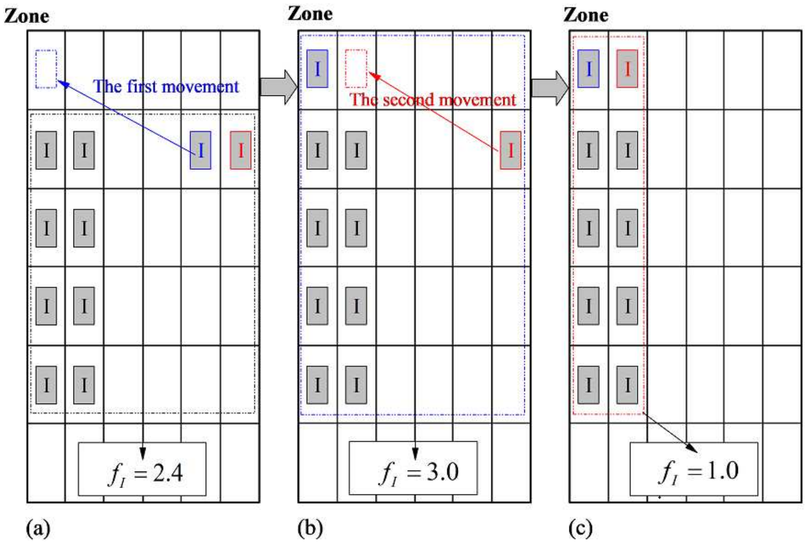


Figure 13 The simple movements of cars for a centralized car layout with minimum dispersion: (a) a scattered car layout, (b) the car layout after the first movement, and (c) the car layout with minimum dispersion

In Section 5.2, we propose an indicator called the attraction degree to reflect the local preference of each location for storing different car groups, and in Section 5.3, we develop the cumulative attraction degree based on the car group (CAD-CG) to identify the efficient movements of cars and exchanges between cars for a centralized car layout.

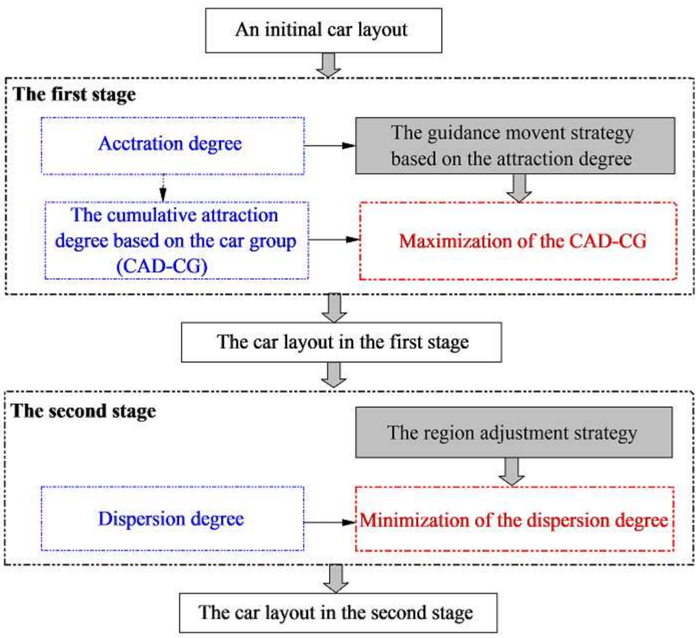


Figure 14 The HTSES framework

Combining the dynamic evolution of the car layout with the identification of the static layout, we present an HTSES for minimizing the dispersion degree in the single phase, which makes the car layout transition from a scattered state to a centralized state. Figure 14 shows the HTSES framework. First, we focus on the guidance exchanges and movements of cars to strengthen the relationships among the cars in the same group; then, we develop a region exchange strategy for further identifying the static car layout with the minimum dispersion degree.

## 5.2 Attraction degree

The attraction degree of location $(r,c)$ for group-$g$ cars, indicated by $l^{g}_{(r,c)}$, is defined as the ratio between the number of group-$g$ cars in neighborhood space $\psi_{(r,c)}$ and a constant, combined with a penalty for deadlock situations. Eqs. (23a) and (23b) present the definitions of the attraction degree and neighborhood space, respectively.

$$l^{g}_{(r,c)} = \sum_{(r',c')\in\psi_{(r,c)}} \sum_{u\in U} (x_u^{(r',c')} \cdot B_{g,u})/8 - M \cdot \sum_{u\in U} B_{g,u} \cdot (\mu^{I}_{u,(r,c)} \cdot \mu^{II}_{u,(r,c)} + \lambda^{I}_{u,(r,c)} \cdot \lambda^{II}_{u,(r,c)}) \quad (23a)$$

$$\psi_{(r,c)} = \{(r',c') \mid \max\{0,r-1\} \le r' \le \min\{r+1,|R|\}, \max\{0,c-1\} \le c' \le \min\{c+1,|R|\}, \text{ and } (r',c') \ne (r,c)\} \quad (23b)$$

The neighborhood space of storage location $(r,c)$ includes the storage locations of its adjacent rows and columns. Figure 15(a) graphically illustrates the neighborhood spaces of four different locations, which are depicted by red frames.

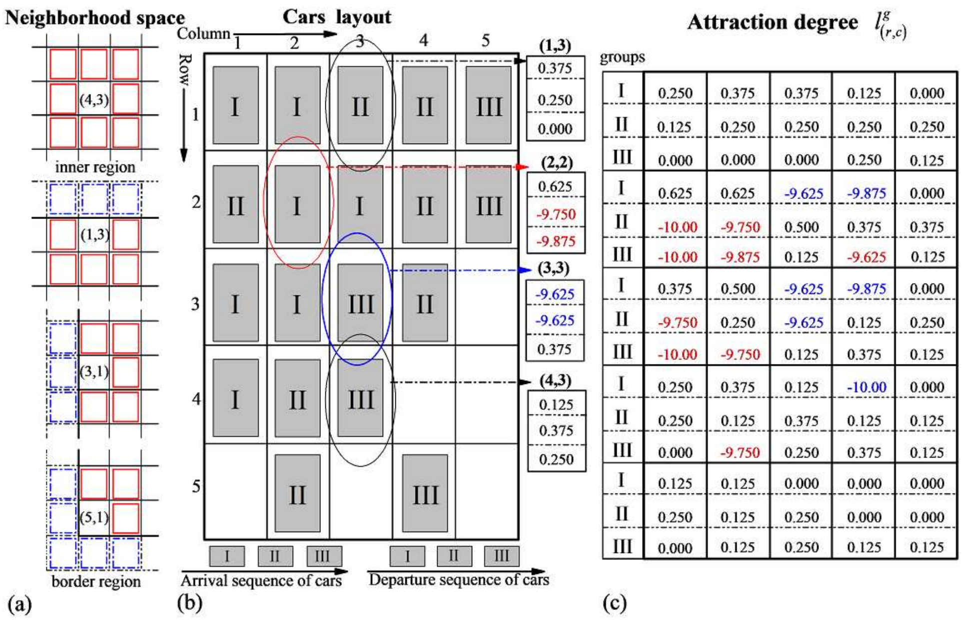


Figure 15 (a) The neighborhood spaces of four different locations; (b) a randomly generated car layout; (c) the attraction degrees of every location for different car groups.

Attraction degree $l^{g}_{(r,c)}$ at location $(r,c)$ for group-$g$ depends on the distribution of cars in its neighborhood. For instance, in the example presented in Figure 15(b), the neighborhood space of location $(4,3)$ consists of eight storage locations, i.e., $\psi_{(4,3)}=\{(3,2),(3,3),(3,4),(4,2),(4,4),(5,2),(5,3),(5,4)\}$. Based on the car distribution at $\psi_{(4,3)}$, the attraction degrees for three car groups can be expressed as $l^{\mathrm{I}}_{(4,3)} = 0.125$, $l^{\mathrm{II}}_{(4,3)} = 0.375$, and $l^{\mathrm{III}}_{(4,3)} = 0.375$ (Figure 15(b)). In the border rows and columns of the zone, the neighborhood space is different from that in the inner locations (Figure 15(a)). For example, the neighborhood space at location $(1,3)$ includes only $\{(1,2),(1,4),(2,2),(2,3),(2,4)\}$. To unify the measure of the attraction degree, a dummy row is added to guarantee that the denominator in Eq. (23a) is constant. Hence, the attraction degrees at border location $(1,3)$ for the three car groups are $l^{\mathrm{I}}_{(4,3)} = 0.375$, $l^{\mathrm{II}}_{(4,3)} = 0.25$, and $l^{\mathrm{III}}_{(4,3)} = 0.0$.

The second part of Eq. (23a) emphasizes the penalty resulting from deadlock situations. Parameter $M$ is a large number called the penalty factor. When a deadlock situation is caused by inserting a group-*g* car into location $(r,c)$, i.e., $\mu^{I}_{u,(r,c)} \cdot \mu^{II}_{u,(r,c)} + \lambda^{I}_{u,(r,c)} \cdot \lambda^{II}_{u,(r,c)} \geq 1$, the penalty is applied to the attraction degree at location $(r,c)$ for group-*g*. In Figure 15(b), if a group-II car is inserted into location $(2,2)$, a deadlock situation resulting from a blocked entrance route occurs based on the arrival sequence of the three car groups (I→II→III). Therefore, the attraction degree of location $(2,2)$ for group-II is $l^{\mathrm{II}}_{(4,3)} = 2/8 - 10 = -9.75$ ($M = 10$). Similarly, due to blocked exit routes, the attraction degree of location $(3,3)$ for group-I is $l^{\mathrm{I}}_{(3,3)} = 3/8 - 10 = -9.625$. Figure 15(c) lists the attraction degree of each location for each car group.

The attraction degree quantifies the degree to which each location is preferred for storing different car groups. A larger attraction degree reflects a higher preference for a car group. Specifically, the penalty reflects the exclusion of the storage location for some specified car groups. Clearly, the attraction degree can provide quantitative guidance for adjusting the car layout in the zone. For example, in Figure 15(c), the attraction degrees of location $(2,1)$ for three car groups are $l^{\mathrm{I}}_{(2,1)} = 0.625$, $l^{\mathrm{II}}_{(2,1)} = -10.0$, and $l^{\mathrm{III}}_{(2,1)} = -10.0$. Therefore, it would be advantageous to substitute a group-I car in another location for the group-II car in location $(2,1)$.

## 5.3 The cumulative attraction degree based on the car group (CAD-CG)

The attraction degree reflects the local preference of a single location for storing a specified car group, and its value is determined by the car distribution of the neighborhood space. Based on local preference, beneficial exchanges or movements of cars can be identified. For instance, Figure 13(a) presents a simple car layout in which seven group-I cars are assigned to a |6*5| zone. Intuitively, this car layout is not satisfactory, and the dispersion degree is approximately 12/7. In Figure 13(a), the attraction degree of location $(4,2)$ for a group-I car is approximately 0.375. Compared to the attraction degree of location $(5,4)$ ($l^{\mathrm{I}}_{(5,4)} = 0.25$), location $(4,2)$ has a high preference for storing a group-I car. After the group-I car at location $(5,4)$ is moved to location $(4,2)$, the attraction degrees at locations $(3,2)$ and $(3,3)$ for group-I increase from 0.5 and 0.625 to 0.625 and 0.75, respectively (Figure 13(b)). Clearly, the attraction degree also reflects the relationships among the assigned cars. Therefore, we introduce an indicator $\mathfrak{L}_g$, called the CAD-CG, to evaluate the relationships among cars of the same group in the zone/zones.

$$\mathscr{L}_g = \sum_{u\in U}\sum_{r\in R}\sum_{c\in C} x_u^{(r,c)} \cdot B_{g,u} \cdot l_{(r,c)}^{g} \qquad \forall\, g \in G \tag{24}$$

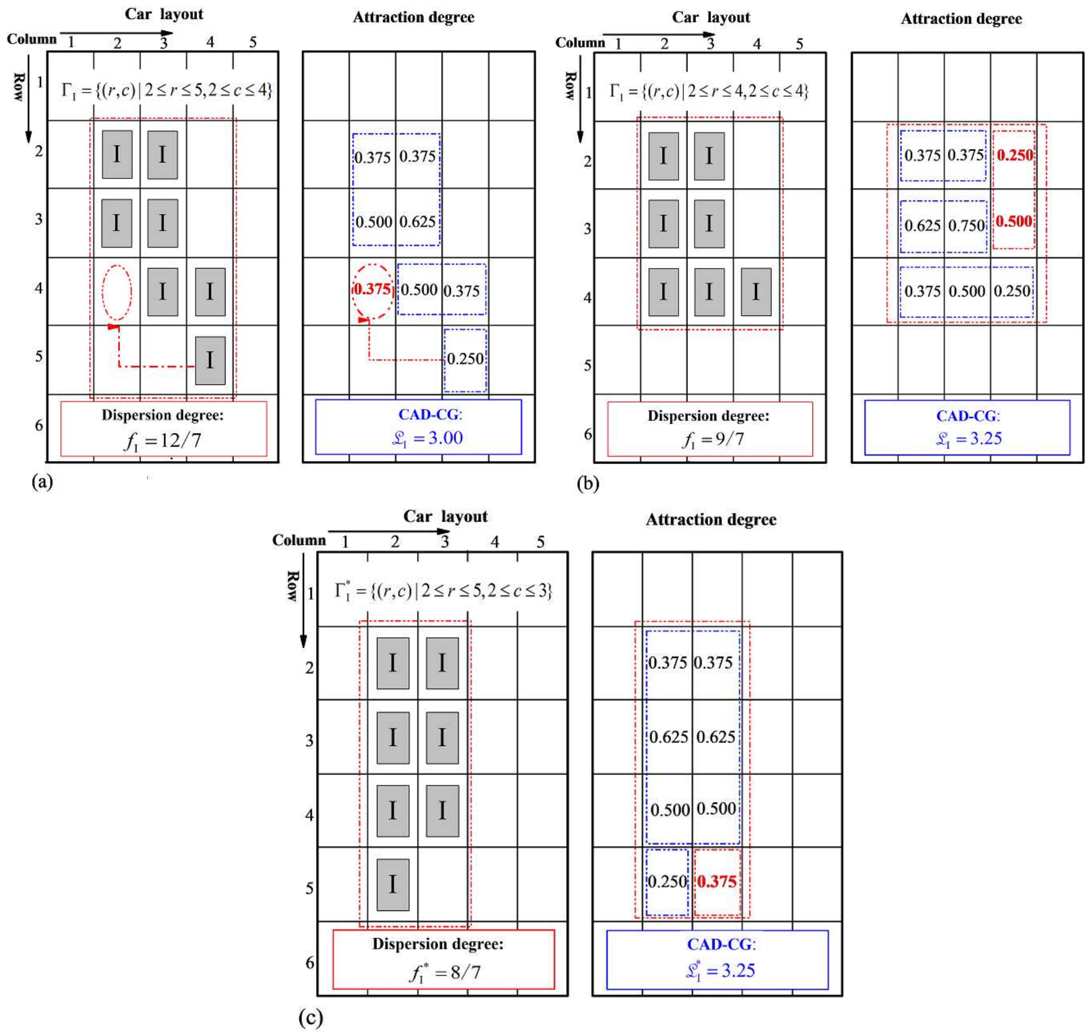


Figure 16 The dispersion degree and the CAD-CG in three car layouts: (a) a feasible car layout, (b) a suboptimal car layout, and (c) the optimal car layout

Based on Eq. 24, in Figure 16(a), the value of $\mathscr{L}_g$ is approximately 3.00, and in Figure 16(b), the value is approximately 3.25. Clearly, the relationships among cars of the same group in Figure 16(b) are stronger than those in Figure 16(a). Hence, maximizing $\mathscr{L}_g$ may be a feasible way to transform the car layout from scattered to centralized.

## 5.4 The HTSES process

As shown in Figure 16(c), although the value of the CAD-CG is the same as that in Figure 16(b), the dispersion degree in the optimal car layout is only 8/7. Clearly, for a centralized car layout, the proposed CAD-CG and dispersion degree originate from different perspectives. The CAD-CG depends on the local correlation among cars of the same group, while the dispersion degree emphasizes the static layout of the car group throughout the entire zone. The CAD-CG cannot be completely substituted for the dispersion degree. The car layout with the minimum dispersion degree must be further identified while maximizing the CAD-CG.

Therefore, we present a clear HTSES: first, it identifies the efficient exchanges or movements of cars to maximize the CAD-CG; second, it develops a regional exchange strategy for obtaining the car layout with the minimum dispersion degree.

- **The first stage: A preferential exchange strategy**

The first stage of the HTSES adopts a preferential exchange strategy for maximizing the total CAD-CG ( $\mathcal{L} = \sum_{g \in G} \mathcal{L}_g$ ). The preferential exchange strategy is described as follows.

- Select the car to be exchanged:

$$(\hat{u}, \hat{g}, \hat{r}, \hat{c}) = Arg \min_{u,g,r,c} \{ l^g_{(r,c)} \mid x^{(r,c)}_u = 1, B_{g,u} = 1, u \in U, r \in R, c \in C \} .$$

- Determine the new location: $(\tilde{r}, \tilde{c}) = Arg \max_{(r,c)} \{ l^{\hat{g}}_{(r,c)} \mid r \in R, c \in C \}$.

Intuitively, the car with the lowest attraction degree has the largest preference for changing its current storage location ( $\hat{u}, \hat{g}, \hat{r}, \hat{c}$ ). Moreover, based on the preferences of all locations for selected group- $\hat{g}$ , i.e., attraction degree $l^{\hat{g}}_{(r,c)}$ , the location with the largest preference for storing group- $\hat{g}$ should be selected as the new location for car $\hat{u}$ . This preferential exchange method is efficient for larger CAD-CG values. The first stage is terminated when the value of $\mathcal{L}$ cannot be improved by any exchanges.

We adopt the example in Figure 17 to describe the first stage of this exchange strategy. Figure 17(a) extracts the attraction degree of each location for the assigned group (the black number in Figure 17(a)). Clearly, the group-II car at location $(2,1)$ ( $l^{\mathrm{II}}_{(2,1)} = -10.00$ ) should be considered as the target. Based on the identification of the attraction degree of all locations for group-II (the blue number in Figure 17(a)), location $(2,3)$ ( $l^{\mathrm{II}}_{(2,3)} = 0.50$ ) has the largest preference for storing the group-II car. Figure 17(b) gives the new car layout after this exchange, in which the value of $\mathcal{L}$ increases from -15.25 to 6.00.

Based on the definition of the attraction degree in Eq. (23a), once a deadlock situation occurs, a penalty is applied to the attraction degree. Cars with a penalty, such as that in location $(2,1)$ in Figure 17(a), have a larger preference for changing their current storage locations. Hence, the proposed exchange strategy can efficiently avoid the development of a deadlock situation.

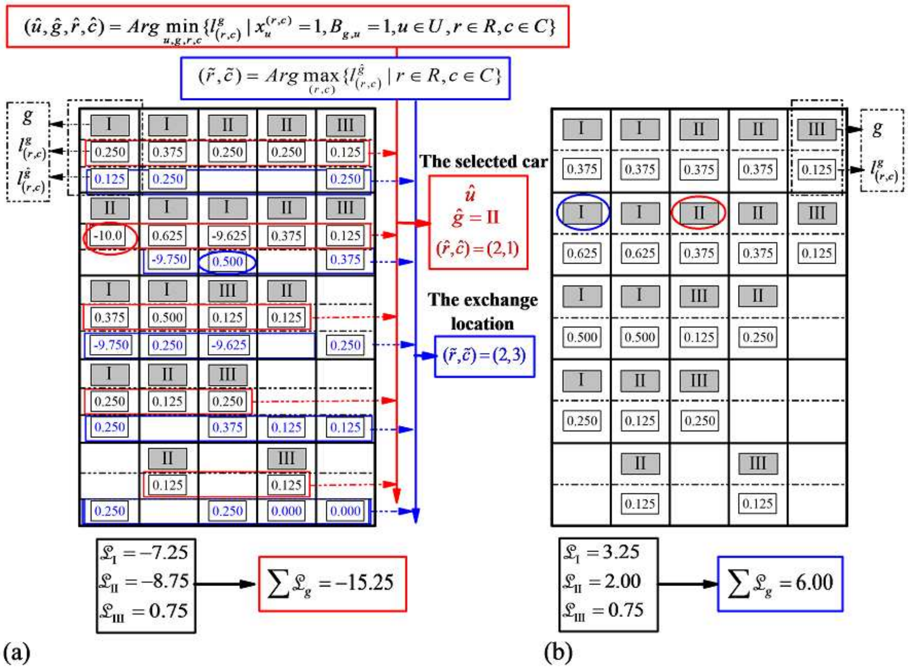


Figure 17 The selection and exchange strategy in the first stage: (a) the car layout before exchange and (b) the car layout after exchange

- **The second stage: A regional exchange strategy**

The second stage in the HTSES focuses on identifying the minimum dispersion degree. The assignment space formed by the car groups in the first stage is divided into compaction and unsaturated regions (Figure 18). The compaction region of group-$g$ denotes the space in which all locations are assigned to group-$g$ cars. The unsaturated region includes idle locations or locations occupied by other groups of cars.

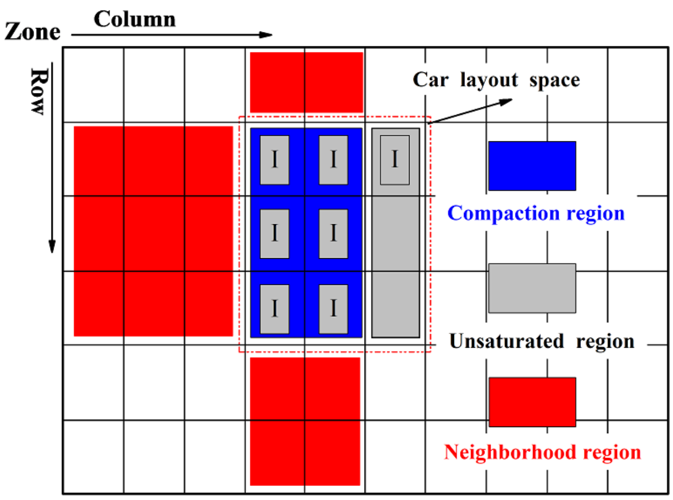


Figure 18 The compaction, unsaturated and neighborhood regions in the assignment space

In the second stage, a simple regional exchange strategy is adopted to minimize the value of $f$ ($f = \sum_{g \in G} f_g$). The cars in the unsaturated region are tentatively moved to or exchanged with a neighborhood region (Figure 18) to generate a new car layout. When the value of $f$ is improved, a regional movement or exchange is accepted. Similar to the first stage, the second stage is terminated when no regional adjustment can improve the total dispersion degrees of all car groups. The pseudocode for the HTSES is presented in Appendix I-1.

# 6. A rolling-horizon approach based on closed-loop feedback

## 6.1 The rolling-horizon approach framework

A large zone in the yard can be shared by cars being loaded into different Ro-Ro ships. Based on constraint (5) in Section 4.2, if cars have no overlap in the time horizon, no storage location conflicts exist. Therefore, we present a rolling-horizon approach based on closed-loop feedback to identify conflicts among cars. The proposed approach is also helpful for reducing the problem scale. The rolling-horizon approach framework is depicted in Figure 19.

The five geometric shapes in Figure 19(a) indicate the adopted symbols when describing the rolling-horizon solution process. The gray rectangle denotes the car layout and dispersion degree. The blue rectangle indicates the adopted method in the rolling-horizon solution process. The red, blue and black ellipses represent three different classes of the car set.

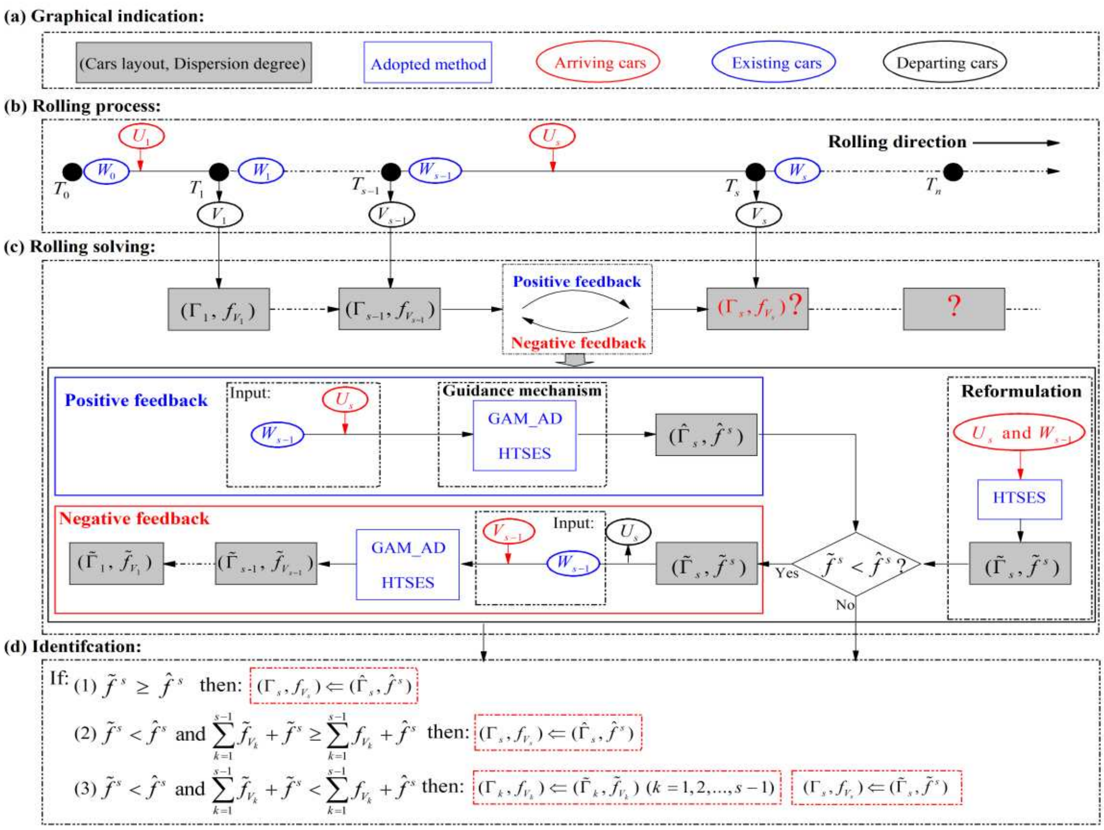


Figure 19 The rolling-horizon approach framework

Based on the departure times or sequences of cars from the zone, the rolling-horizon process is discretized to multiple phases, as indicated by set $T$ ($T = \{T_1, \ldots, T_s, \ldots, T_n\}$). In Figure 19(b), set $V_s$, indicated by the black ellipse, records the departing cars at phase $T_s$ ($V_s = \{u \mid t_u^d = T_s,\ u \in U\}$). The arriving cars at time region $[T_{s-1}, T_s)$ are denoted by set $U_s$ ($U_s = \{u \mid T_{s-1} \le t_u^a < T_s, u \in U\}$), and set $W_s$ indicates the existing cars in the zone at time interval $(T_{s-1}, T_s)$, i.e., $W_s = \{u \mid u \in U, t_u^a < T_{s-1}, t_u^d > T_{s-1}\}$.

Along the rolling direction, the rolling-horizon approach gradually captures the layout of departing cars for each discrete time point. In Figure 19(c), $\Gamma_s$ and $f_{V_s}$ denote the layout of the departing car groups and the value of the dispersion degree at time $T_s$, respectively. We adopt the closed-loop feedback heuristic algorithm to generate car layout $\Gamma_s$ at phase $T_s$. The positive feedback emphasizes the guidance effect of an existing car layout in set $W_s$ on the arriving cars in set $U_s$. Moreover, the negative feedback triggered by the reformulation mechanism is used to identify the impact of the arriving cars in set $U_s$ on the existing car layout in the zone. $\hat{\Gamma}_s$ and $\tilde{\Gamma}_s$ indicate car layouts generated by two different feedback mechanisms. $\hat{f}_s$ and $\tilde{f}_s$ represent the dispersion degrees in car layouts $\hat{\Gamma}_s$ and $\tilde{\Gamma}_s$, respectively. Finally, the criterion provided in Figure 19(d) is used to identify the effectiveness of the positive and negative feedback mechanisms. The closed-loop feedback heuristic will be discussed in detail in Sections 6.2 and 6.3.

## 6.2 Positive feedback based on the guidance mechanism

During the planned time period, positive feedback guides the assignment of the arriving cars in set $U_s$ based on the existing car layout in set $W_s$ in the zone. The guidance mechanism originates from the preferences of the storage locations for the arriving cars. Based on the existing car layout in set $W_s$, the attraction degrees of each location for different car groups can be easily calculated. Arriving car $\hat{u}$ in group-$\hat{g}$ ($B_{\hat{g},\hat{u}} = 1$) is assigned to the idle location with the largest preference for storing group-$\hat{g}$. Here, a guidance assignment mechanism based on the attraction degree **(GAM_AD)** is proposed to show the preferences of the idle locations for storing different car groups.

$$x_{\hat{u}}^{(\hat{r},\hat{c})} = 1 \text{ if: } \hat{u} \in U_s,\ B_{\hat{g},\hat{u}} = 1 \text{ and } (\hat{r},\hat{c}) = Arg\max_{(r,c)}\{l_{(r,c)}^{\hat{g}} \mid \exists\, v \in W_s,\ x_v^{(r,c)} = 0, r \in R, c \in C\}$$

Once car $\hat{u}$ is inserted into location $(\hat{r},\hat{c})$, the attraction degrees of each location for different car groups will be updated based on the current car layout. Cars in set $U_s$ will be inserted into the zone based on the gradual updating of the attraction degree.

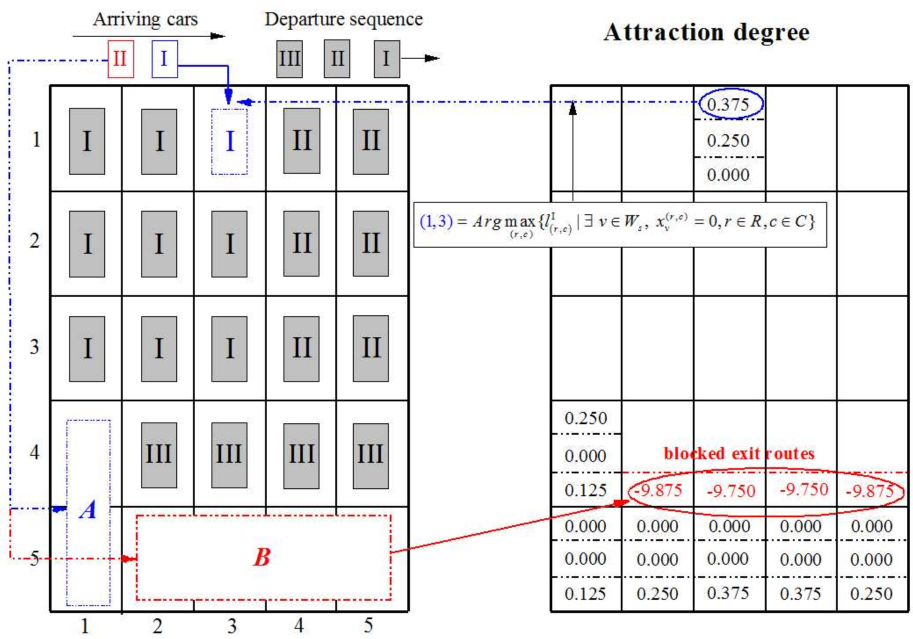


Figure 20 The competition between arriving cars for storage locations

However, the order assignment based on the GAM_AD emphasizes only the preferences of idle locations for storing different car groups. The competition among the cars in set $U_s$ for storage locations is omitted in the above assignment process. For example, in Figure 20, an arriving group-I car is assigned to location $(1,3)$ based on the preferences of locations for storing group-I, and the dispersion degree of group-I cars is approximately 1.00. An arriving group-II car can be assigned to a location in only region A or B. If it is assigned to location $(4,1)$, then the dispersion degree of group-II is approximately 2.857. Clearly, the car layout of group-II deviates considerably from the centralized layout. If region B is selected, then the exit routes of group-III cars are blocked (Figure 20). If the storage locations of arriving group-I and group-II cars are exchanged, then the total dispersion degrees of the two car groups are reduced from 4.857 to 3.619. Hence, arriving group-I and group-II cars compete for location $(1,3)$.

Therefore, when positive feedback occurs, the GAM_AD assigns only initial locations for arriving cars. The HTSES should be further adopted to improve the centralized layout of every car group. Notably, the cars in set $W_s$ cannot be exchanged or moved in the HTSES.

## 6.3 Negative feedback triggered by the reformulation mechanism

Positive feedback emphasizes the guidance effect of the existing car layout on arriving cars. However, the neighborhood space of the existing car layout is not guaranteed to have sufficient idle locations to assign arriving cars. In the example depicted in Figure 21(a), the neighborhood space of the existing layout of group-I cars has sufficient idle locations for assigning three arriving group-I cars. The centralized layout of the group-I cars can be developed based on the guidance assignment mechanism. However, in Figure 21(b), the locations in region A cannot be occupied by the arriving group-I cars due to the blocked entrance routes. The three arriving group-I cars are assigned to locations in region B or C. Clearly, the existing car layout in Figure 21(b) restrains the development of the centralized layout.

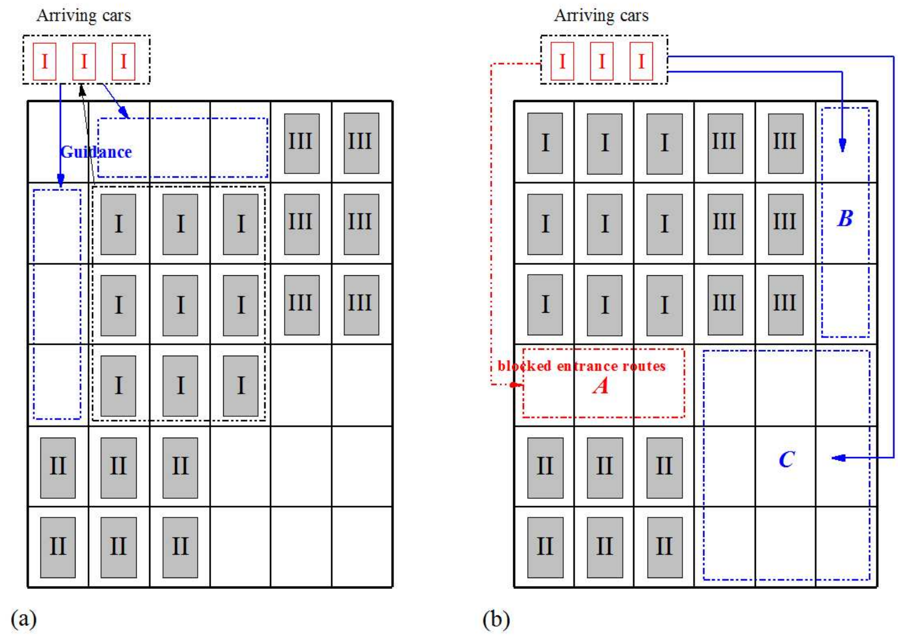


Figure 21 The arriving car assignment based on two existing car layouts

Therefore, during the planned time period, negative feedback triggered by the reformulation mechanism is used to identify the impact of arriving cars on the existing car layout. For reformulation at $T_s$, all cars in sets $W_s$ and $U_s$ are reassigned to the zone. Notably, set $W_s$ may include some cars in set $W_0$. However, the reformulation of the car locations does not include the cars in set $W_0$ because they arrived at the yard before the planned time period (Figure 19).

We adopt $\hat{\Gamma}_s$ to indicate the car layout generated by the GAM_AD and HTSES in the positive feedback process, and we adopt $\tilde{\Gamma}_s$ to indicate the reformulated car layout generated by the HTSES. Clearly, if the dispersion degree in $\tilde{\Gamma}_s$ is smaller than that in $\hat{\Gamma}_s$, i.e., $\tilde{f}_s < \hat{f}_s$, then the reformation mechanism at time $T_s$ can efficiently improve the current centralized car layout. Due to the reformulated car layout in set $W_s$, negative feedback requires the layout of the car groups to be reformulated before time $T_s$. As shown in Figure 19(c), the cars in set $U_s$ are removed from $\tilde{\Gamma}_s$. The GAM_AD and HTSES are adopted to reassign the departing car groups in set $V_{s\text{-}1}$, and the reformulated car layout $\tilde{\Gamma}_{s-1}$ at time $T_{s-1}$ is generated. Negative feedback is terminated when car layout $\tilde{\Gamma}_1$ at time $T_1$ is reformulated. When the centralized performance of the reformulated car layout is better than that of the car layout in the positive feedback process, i.e., $\sum_{k=1}^{s-1}\tilde{f}_{V_k}+\tilde{f}_s<\sum_{k=1}^{s-1}\hat{f}_{V_k}+\hat{f}_s$, negative feedback is efficient, and the reformulated car layout is accepted as the current car assignment plan (Figure 19(c)).

# 7. Numerical experiments

Next, we illustrate the characteristics of the proposed model and the performance of the method from the following three perspectives based on a series of numerical experiments: (1) the performance of the HTSES for the assignment of cars in the single phase, (2) the performance of the rolling-horizon approach based on closed-loop feedback for the car assignment plan, and (3) a comparison between AR-CT and AR-CG based on real-world scenarios.

The CPLEX 12.6 commercial solver is adopted to obtain the optimal solution to small-scale numerical examples. The algorithms presented in Sections 5 and 6 are implemented in the C++ language and executed on a PC with a Windows 7 operating system equipped with an Intel E5-4620 2.2 GHz processor and 16 GB of RAM.

## 7.1 HTSES performance

As shown in Figure 19, the HTSES is embedded in the rolling-horizon approach based on closed-loop feedback. The performance of the HTSES determines the efficiency of the rolling-horizon approach. Hence, this section focuses on HTSES performance in terms of solution quality and computational time.

Table 2 presents 12 random scenarios. The second column in Table 2 presents the number of rows and columns in one zone in the yard. The 4 groups of cars are assigned to the zone in each scenario, and the numbers of cars in each group are given in the third column. The arrival and departure (loading) sequences of car groups are presented in the fourth and fifth columns, respectively. The HTSES is applied when $K_{u,v}=1$, i.e., $x_u^{(r,c)}+x_v^{(r,c)}\le 1$. Hence, in these scenarios, previously arriving cars cannot depart from the yard before the latest cars arrive at the yard. For example, in the first scenario, the departure time of group-I cars is after the arrival time of group-II cars, i.e., $t_{\mathrm{I}}^d>t_{\mathrm{II}}^a$.

Table 3 presents the results of the proposed model obtained by the CPLEX 12.6 solver for 12 scenarios. The computational time of the CPLEX solver is set to 24 hours. The optimal solution is obtained in only four scenarios (scenarios 1-4).

The HTSES has good efficiency in terms of solution quality and computational time. In 6 scenarios (scenarios 1-6), the results obtained by the HTSES are the same as those obtained by the

CPLEX 12.6 solver. As the problem scale increases, the quality of the HTSES solutions is better than that of the solutions obtained by the CPLEX 12.6 solver. As presented in Table 3, the average gap between the solutions produced by HTSES and the lower bound is approximately 0.073, while for the CPLEX 12.6 solver, the gap is approximately 0.126. Moreover, the HTSES demonstrates excellent computational efficiency; its required computational time in the 12 scenarios does not exceed 2 seconds.

Table 2: Parameters in 12 random scenarios

| Scenario (#) | Zone scale (\|R\|*\|C\|) | Car group and number | Arrival sequence | Departure sequence |
|---|---|---|---|---|
| 1 | 5*3 | I(7)/II(3)/III(3)/IV(2) | III→IV→I→II | I→III→IV→II |
| 2 | | I(9)/II(4)/III(1)/IV(1) | I→IV→II→III | IV→I→II→III |
| 3 | 5*4 | I(11)/II(2)/III(3)/IV(4) | IV→III→I→II | I→IV→II→III |
| 4 | | I(9)/II(7)/III(2)/IV(2) | I→II→IV→III | IV→I→II→III |
| 5 | 5*5 | I(11)/II(5)/III(8)/IV(1) | I→II→III→IV | I→III→II→IV |
| 6 | | I(10)/II(5)/III(7)/IV(3) | I→IV→II→III | I→II→IV→III |
| 7 | 5*6 | I(16)/II(7)/III(1)/IV(6) | I→II→III→IV | II→I→IV→III |
| 8 | | I(16)/II(3)/III(9)/IV(2) | I→II→III→IV | III→I→IV→II |
| 9 | 5*7 | I(13)/II(9)/III(6)/IV(7) | IV→II→I→III | III→I→IV→II |
| 10 | | I(11)/II(7)/III(8)/IV(9) | I→II→IV→III | II→IV→I→III |
| 11 | 5*8 | I(4)/II(8)/III(21)/IV(7) | I→II→IV→III | IV→I→III→II |
| 12 | | I(7)/II(7)/III(18)/IV(8) | II→III→I→IV | II→I→IV→III |

Table 3: Numerical results from the CPLEX 12.6 solver and the HTSES for the scenarios in Table 2

| # | CPLEX 12.6 solver | | | | HTSES | | |
|---|---|---|---|---|---|---|---|
| | LB | UB | $\text{gap}^1$ | CPU time | $f$ | CPU time | $\text{gap}^2$ |
| 1 | 4.111 | 4.111 | 0.000 | 11.5/s | 4.111 | 0.17/s | 0.000 |
| 2 | 4.286 | 4.286 | 0.000 | 259.2/s | 4.286 | 0.21/s | 0.000 |
| 3 | 4.091 | 4.091 | 0.000 | 10.8/h | 4.091 | 0.49/s | 0.000 |
| 4 | 4.286 | 4.286 | 0.000 | 17.8/h | 4.286 | 0.35/s | 0.000 |
| 5 | 4.091 | 4.343 | 0.062 | 24.0/h | 4.343 | 0.63/s | 0.062 |
| 6 | 4.143 | 4.476 | 0.083 | 24.0/h | 4.476 | 1.68/s | 0.083 |
| 7 | 4.143 | 4.411 | 0.065 | 24.0/h | 4.393 | 1.78/s | 0.060 |
| 8 | 4.000 | 4.843 | 0.211 | 24.0/h | 4.593 | 1.72/s | 0.148 |
| 9 | 4.077 | 4.696 | 0.152 | 24.0/h | 4.582 | 1.19/s | 0.124 |
| 10 | 4.091 | 4.756 | 0.163 | 24.0/h | 4.595 | 2.07/s | 0.123 |
| 11 | 4.000 | 5.048 | 0.262 | 24.0/h | 4.601 | 1.92/s | 0.150 |
| 12 | 4.000 | 6.063 | 0.516 | 24.0/h | 4.536 | 1.74/s | 0.134 |
| Average | | | 0.126 | | | | 0.073 |

Note: LB: lower bound; UB: upper bound. $\text{gap}^1$ = (UB-LB)/LB; $\text{gap}^2$ = ($f$-LB)/LB.

In Figure 22, we present the static assignment of cars obtained by the CPLEX 12.6 solver and the HTSES for scenario 7. Compared to the solution from the CPLEX 12.6 solver, the total dispersion degrees of all car groups are small (approximately 4.393). Additionally, the required computational time is only approximately 1.78 seconds. Clearly, this performance ensures that the HTSES can be regarded as the basic sub method in the rolling-horizon approach based on closed-loop feedback.

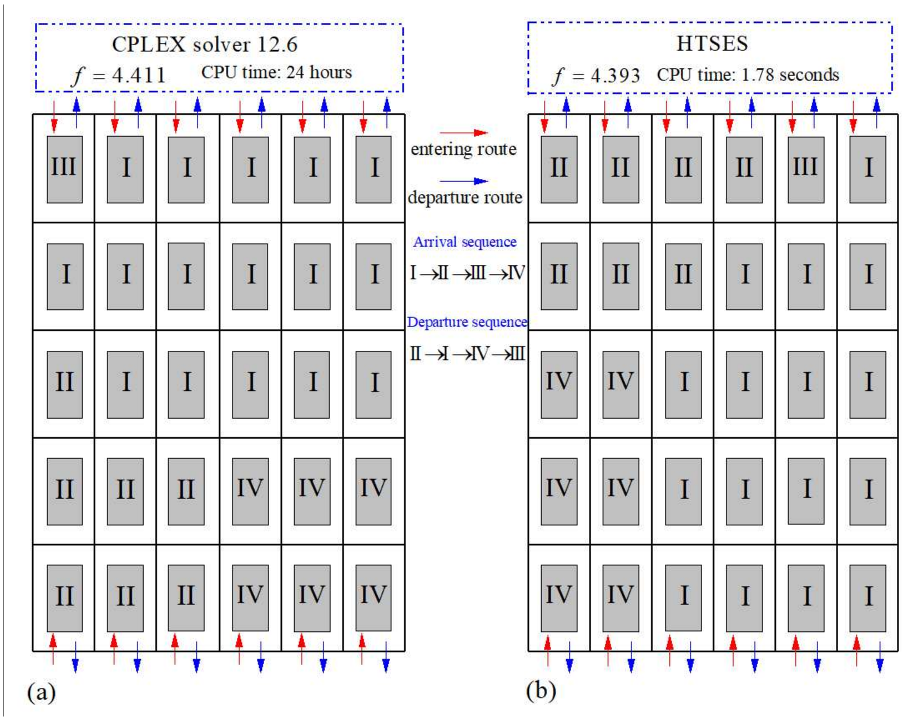


Figure 22 Two car layouts in scenario 7: (a) layout based on the CPLEX 12.6 solver and (b) layout based on the HTSES

## 7.2 Rolling-horizon approach performance

The rolling-horizon approach separates the entire time horizon into different phases based on the departure times of car groups. Positive and negative feedback strengthen the relationships among different car groups. Table 4 details five groups of experiments in which the scale of the zone is increased from |5*3| to |5*7|; these experiments are used to evaluate the performance of the rolling-horizon approach. Each group of experiments includes 3 scenarios, and the number of cars in each scenario is gradually increased. The fourth and fifth columns in Table 4 give the number of car groups and their arrival and departure sequences in each scenario, respectively.

Table 4: Parameters in 15 random scenarios

| # | Zone scale | Car number | Group number | Arrival (A.) and Departure (D.) sequence of cars |
|---|---|---|---|---|
| 1 | | 19 | 3 | A.{I(2),II(7),III(3)}→D.{II(7)}→A.{I(2),III(3)}→D.{III(6)}→A.{I(2)}→D.{I(7)} |
| 2 | 5*3 | 24 | 4 | A.{I(4),II(4),III(2)}→D.{II(4)}→A.{I(3),IV(3)}→D.{I(7)}→A.{III(4)}→D.{III(6)}→A.{IV(4)}→ D.{IV(7)} |
| 3 | | 40 | 5 | A.{I(2),II(6),III(2),IV(2)}→D.{II(6)}→A.{I(2),IV(2),V(3)}→D.{IV(4)}→A.{I(2),V(4)}→ D.{V(7)}→A.{I(3),III(3)}→D.{I(9)}→A.{III(2)}→D.{III(7)} |
| 4 | | 25 | 4 | A.{I(3),II(3),III(3)}→D.{II(3)}→A.{I(2),III(4)}→D.{III(7)}→A.{I(3),IV(3)}→D.{I(9)}→ A.{IV(4)}→D.{IV(7)} |
| 5 | 5*4 | 32 | 4 | A.{I(4),II(4),III(4),IV(2)}→D.{II(4)}→A.{I(4),III(5),IV(3)}→D.{III(9)}→A.{I(4), IV(2)}→ D.{I(12),IV(7)} |
| 6 | | 38 | 5 | A.{I(3),II(4),IV(3),V(2)}→D.{II(4)}→A.{I(3),III(3),IV(3),V(2)}→D.{IV(6)}→A.{I(2),III(3)}→ D.{III(6)}→A.{I((3),V(5))}→D.{V(9)}→A.{I(2))}→D.{I(13)} |

| | | | | |
|---|---|---|---|---|
| 7 | 5*5 | 33 | 4 | A.{I(3),II(4),III(3),IV(3)}→D.{II(4)}→A.{I(3),III(3),IV(4)}→D.{IV(7)}→A.{I(3), III(3)}→ D.{III(9)}→A.{ I(4)}→D.{I(13)} |
| 8 | | 38 | 4 | A.{I(3),II(8),III(3),IV(4)}→D.{II(8)}→A.{I(3),III(3),IV(4)}→D.{IV(8)}→A.{I(3), III(3)}→ D.{I(9)}→A.{III(4)}→D.{III(13)} |
| 9 | | 45 | 5 | A.{I(3),II(6),III(3),V(3)}→D.{II(6)}→A.{I(3),III(3),IV(4),V(3)}→D.{III(6)}→A.{IV(3),V(3)}→ D.{V(9)}→A.{I(3),IV(4)}→D.{IV(11)}→A.{I(4)}→D.{I(13)} |
| 10 | 5*6 | 40 | 4 | A.{I(7),II(4),III(11)}→D.{I(7),III(11)}→A.{II(5),IV(7)}→D.{II(9)}→A.{IV(6)}→D.{IV(13)} |
| 11 | | 45 | 5 | A.{I(3),II(6),III(4),IV(4),V(2)}→D.{II(6)}→A.{I(3),III(3),IV(4),V(2)}→D.{IV(8)}→A.{IV(3), V(3)}→D.{V(7)}→A.{I(3),III(3)}→D.{I(12)}→A.{III(2))}→D.{III(12)} |
| 12 | | 60 | 6 | A.{I(3),II(6),III(3),IV(3),V(3),VI(3)}→D.{II(6)}→A.{I(3),III(3),IV(2),V(4),VI(3)}→D.{V(6)}→ A.{IV(2),VI(4)}→D.{VI(10)}→A.{I(3),III(3),IV(4)}→D.{IV(11) →A.{I(4)}→D.{I(13)}→ A.{III(4))}→D.{III(13)} |
| 13 | 5*7 | 52 | 5 | A.{I(4),II(6),III(2),IV(4)}→D.{II(6)}→A.{I(4),III(4),IV(3),V(3)}→D.{IV(7)}→A.{I(4),III(5), V(3)}→D.{I(12)}→A.{V(5)}→D.{V(11)}→A.{III(5)}→D.{III(16)} |
| 14 | | 62 | 5 | A.{I(4),II(8),III(5),IV(4)}→D.{II(8)}→A.{III(5),IV(5),V(4)}→D.{IV(9)}→A.{I(4),III(5),V(4)}→ D.{III(15)}→A.{I(4),V(5)}→D.{I(12)}→A.{V(5))}→D.{V(18)} |
| 15 | | 70 | 6 | A.{I(3),II(8),III(6),VI(3)}→D.{II(8)}→A.{I(3),III(5),V(3),VI(2)}→D.{III(11)}→A.{IV(4),V(4), VI(3)}→D.{VI(8)}→A.{I(3),IV(4),V(5)}→D.{V(12)}→A.{I(4),IV(4)}→D.{I(13)}→A.{IV(6)} →D.{IV(18)} |

Table 5: Numerical results from the CPLEX 12.6 solver and the rolling-horizon approach for the scenarios in Table 4

| # | CPLEX 12.6 solver | | | | Rolling-horizon approach | | | | | |
|---|---|---|---|---|---|---|---|---|---|---|
| | LB | UB | gap[1] | CPU time | $f$ | CPU time | gap[2] | $N_{rolling}$ | $m_{neg}$ | $m_{neg}^{eff}$ |
| 1 | 3.286 | 3.286 | 0.000 | 12.6/h | 3.286 | 1.49/s | 0.000 | 3 | 1 | 1 |
| 2 | 4.286 | 4.286 | 0.000 | 13.9/h | 4.286 | 1.98/s | 0.000 | 4 | 0 | 0 |
| 3 | 5.397 | 5.397 | 0.000 | 21.5/h | 5.397 | 6.46/s | 0.000 | 5 | 2 | 1 |
| 4 | 4.286 | 4.286 | 0.000 | 16.8/h | 4.286 | 3.97/s | 0.000 | 4 | 1 | 1 |
| 5 | 4.143 | 4.730 | 0.142 | 24.0/h | 4.393 | 5.83/s | 0.060 | 3 | 1 | 1 |
| 6 | 5.077 | 5.564 | 0.096 | 24.0/h | 5.265 | 7.97/s | 0.037 | 5 | 1 | 1 |
| 7 | 4.220 | 4.408 | 0.045 | 24.0/h | 4.297 | 5.47/s | 0.018 | 4 | 1 | 1 |
| 8 | 4.077 | 4.265 | 0.046 | 24.0/h | 4.154 | 7.72/s | 0.019 | 4 | 1 | 1 |
| 9 | 5.168 | 5.912 | 0.144 | 24.0/h | 5.578 | 10.36/s | 0.079 | 5 | 2 | 1 |
| 10 | 4.334 | 4.499 | 0.038 | 24.0/h | 4.387 | 5.33/s | 0.012 | 4 | 0 | 0 |
| 11 | 5.143 | 5.679 | 0.024 | 24.0/h | 5.268 | 9.85/s | 0.024 | 5 | 2 | 1 |
| 12 | 6.388 | 7.685 | 0.203 | 24.0/h | 7.381 | 13.63/s | 0.155 | 6 | 2 | 1 |
| 13 | 5.091 | 5.984 | 0.175 | 24.0/h | 5.546 | 11.25/s | 0.089 | 5 | 1 | 0 |
| 14 | 5.000 | 5.645 | 0.129 | 24.0/h | 5.236 | 13.81/s | 0.047 | 5 | 1 | 1 |
| 15 | 6.168 | 6.873 | 0.114 | 24.0/h | 6.676 | 18.21/s | 0.082 | 6 | 3 | 3 |
| Average (scenarios 5~15) | | | 0.105 | | | | 0.057 | | | |

Note: (1) LB: lower bound; UB: upper bound. (2) gap[1] = (UB-LB)/LB; gap[2] = ($f$-LB)/LB. (3) $N_{rolling}$ : the numbers of rolling phases. (4) $m_{neg}$ and $m_{neg}^{eff}$ : the numbers of negative feedback and efficient negative feedback.

Optimal solutions can be obtained by the CPLEX 12.6 solver for some small-scale experiments, such as scenarios 1-4. Despite their small scale, the computational time of the CPLEX 12.6 solver for these optimal solutions exceeds 12 hours. Compared to the CPLEX 12.6 solver, the rolling-horizon approach provides the optimal solution very quickly. For example, in scenario 1, the computational time with the CPLEX 12.6 solver is approximately 12.8 hours, while the rolling-horizon approach requires only approximately 1.49 seconds. As the zone scale increases, it is difficult for the CPLEX 12.6 solver to obtain optimal solutions within a finite time. The computational times from scenario 5 to scenario 15 are set to 24 hours. The numerical results show that the results obtained by the rolling-horizon approach are better than those obtained by the

CPLEX 12.6 solver for these 11 scenarios. For the feasible solutions obtained by the CPLEX 12.6 solver, the average gap between the lower and upper bounds is approximately 0.105 (gap[1]), while for the rolling-horizon approach, the gap is only 0.057 (gap[2]). Additionally, the average computational time of the rolling-horizon approach is approximately 9.95 seconds in these scenarios, which indicates that the rolling-horizon approach can obtain a satisfactory car assignment plan within an acceptable computational time.

The rolling-horizon approach consumes more time in some small-scale scenarios than in some medium-scale scenarios. For example, the number of cars assigned to the 5*3 zone is 33 in scenario 3, and the computational time is approximately 6.46 seconds. However, the rolling-horizon approach requires little time in some larger zones. For instance, in scenario 10, only 5.33 seconds are required to assign 40 cars to a 5*6 zone. Notably, the time consumption of the rolling-horizon approach is closely related to its rolling optimization process.

In the rolling approach based on closed-loop feedback, positive feedback emphasizes the guidance effect of the existing car layout on arriving cars, and negative feedback reflects the influence of arriving cars on the existing car layout. As shown in Figure 19, when negative feedback is applied, the car layout is reformulated until the first phase is complete. Clearly, more time is needed if negative feedback occurs. However, efficient negative feedback must satisfy two conditions: (1) the reformulation assignment results in an improved car layout, which triggers the negative feedback process; and (2) the total dispersion degrees of the departing car groups in all reformulated phases should be lower than that in the positive feedback process.

The ninth, tenth, and eleventh columns in Table 5 list the numbers of rolling phases ( $N_{rolling}$ ), the occurrences of negative feedback ( $m_{neg}$ ), and efficient negative feedback ( $m_{neg}^{eff}$ ), respectively. Clearly, the number of occurrences of negative feedback is less than that in the rolling phases because the triggering condition cannot be satisfied. The guidance assignment mechanism in positive feedback can provide the most rational car layout possible. For example, in scenario 10, no negative feedback is applied in the four rolling phases.

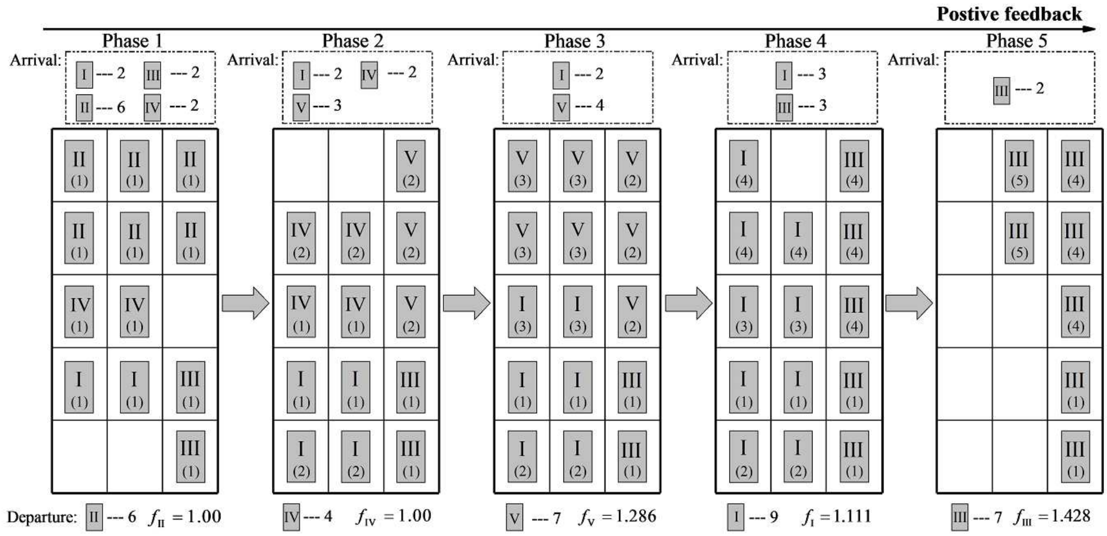

Postive feedback
Phase 1
Phase 2
Phase 3
Phase 4
Phase 5
Arrival:
Departure:


(a)

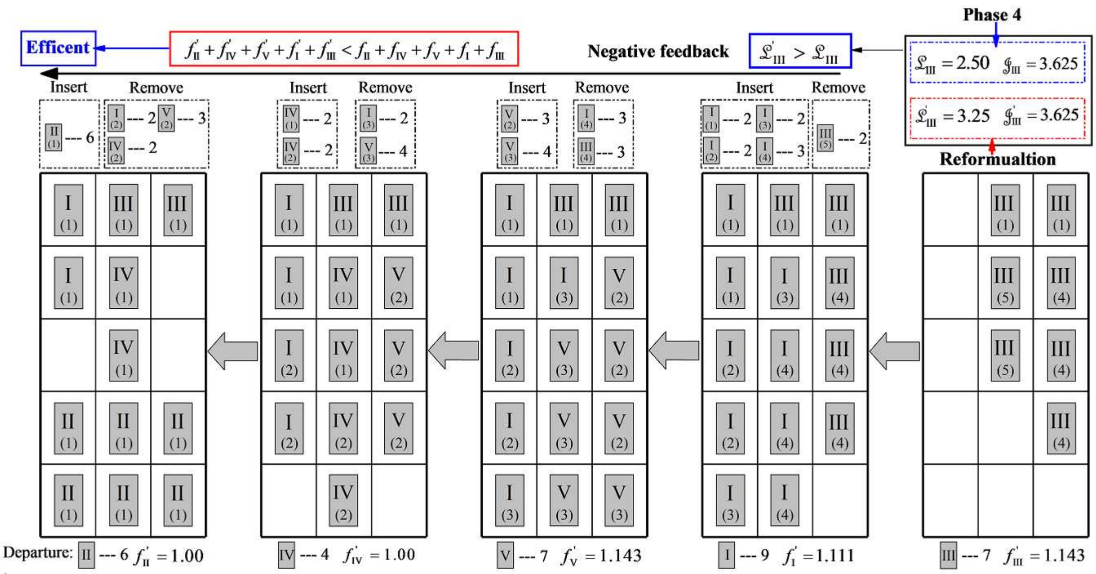

Efficent
Negative feedback
Phase 4
Reformualtion
Insert
Remove
Departure:


(b)

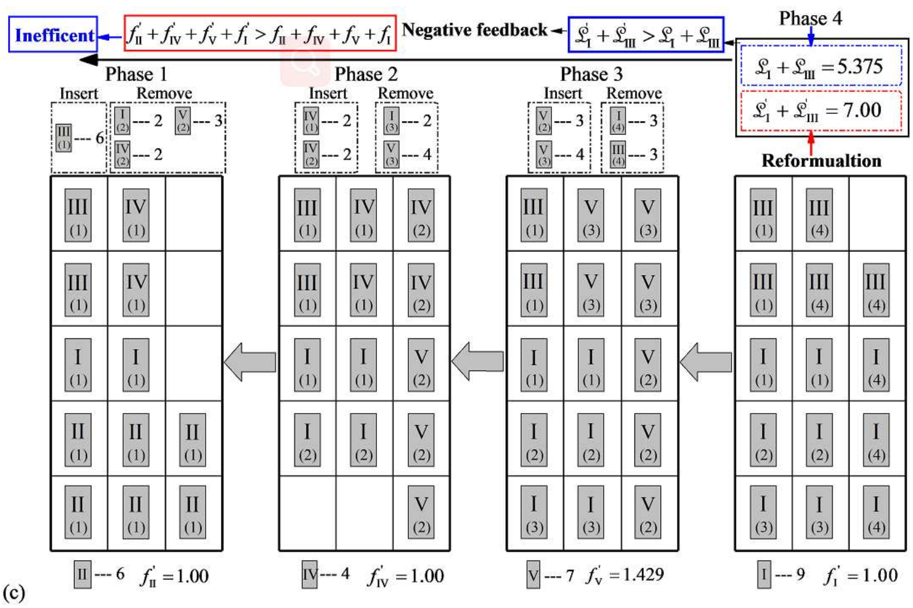

Inefficent
Negative feedback
Phase 4
Reformualtion
Phase 1
Phase 2
Phase 3
Insert
Remove


(c)

Figure 23 The rolling process in scenario 5: (a) the positive feedback process, (b) the negative feedback process originating from phase 5, and (c) the negative feedback process originating from phase 4

However, negative feedback remains necessary to avoid a local optimum during the rolling process. We adopt scenario 3 as an example to illustrate the necessity of negative feedback during the rolling optimization process. The number of cars assigned to the zone is 33, and the zone includes five car groups. The arrival and departure sequences are presented in Table 4. The rolling process is divided into five phases. The results show that two negative feedback processes are executed in the rolling process and that one efficient negative feedback process occurs in the last phase. Figure 23(a) presents the car layout in the positive feedback process based on the guidance assignment mechanism. In the last phase, the HTSES reformulates the car layout of group-III, and a better layout of group-III triggers the negative feedback process. Figure 23(b) presents the reformulated car layout from the fourth phase to the first phase. Comparing the total dispersion degrees in the two classes of car layouts, i.e., $f_{\mathrm{II}}^{'} + f_{\mathrm{IV}}^{'} + f_{\mathrm{V}}^{'} + f_{\mathrm{I}}^{'} + f_{\mathrm{III}}^{'} < f_{\mathrm{II}} + f_{\mathrm{IV}} + f_{\mathrm{V}} + f_{\mathrm{I}} + f_{\mathrm{III}}$, we find that the negative feedback occurring in the fifth phase is efficient.

In scenario 3, negative feedback also occurs in the fourth phase. Similar to the above example, the car layout is reformulated by the HTSES (Figure 23(c)), and the better dispersion degree triggers the negative feedback process, as depicted in Figure 23(c). However, this negative feedback process is inefficient because the total dispersion degrees of the departing car groups are not improved, i.e., $f_{\mathrm{II}}^{'} + f_{\mathrm{IV}}^{'} + f_{\mathrm{V}}^{'} + f_{\mathrm{I}}^{'} > f_{\mathrm{II}} + f_{\mathrm{IV}} + f_{\mathrm{V}} + f_{\mathrm{I}}$.

## 7.3 A comparison of AR-CT and AR-CG

For a small zone, a rational car layout can be easily obtained based on experience. The car assignment plans in Figure 23(a) and (c) can also be accepted by administrators. However, as the zone scale increases, experience may be lacking. Section 3.3 notes that AR-CT may not be a good assignment rule and may result in a scattered car layout following the ship-loading process and increase the risk of insufficient use of storage resources. In this section, we apply AR-CT and AR-CG to real scenarios based on the Shanghai Haitong Ro-Ro Terminal. The scale of the zone is increased from |20*10| to |38*16|. The number of assigned cars is increased from 120 to 540 in 12 random scenarios. These cars are classified into ten types based on their suppliers, brands, versions, etc., and there are six car groups based on the Ro-Ro ship stowage plan.

Table 6: A comparison between AR-CT and AR-CG

| # | Type number | Group number | Lower bound | Zone scale | Car number | AR-CT | | | AR-CG | | |
|---|---|---|---|---|---|---|---|---|---|---|---|
| | | | | | | $f$ | gap | CPU time /s | $f$ | gap | CPU time /s |
| 1 | | | | | 120 | 31.656 | 4.276 | 0.015 | 6.609 | 0.102 | 39.238 |
| 2 | 10 | 6 | 6 | 20*10 | 150 | 28.360 | 3.727 | 0.015 | 7.224 | 0.204 | 52.431 |
| 3 | | | | | 180 | 29.691 | 3.949 | 0.015 | 6.995 | 0.166 | 65.642 |

| | | | | | | | | |
|---|---|---|---|---|---|---|---|---|
| 4 | | 240 | 35.161 | 4.860 | 0.015 | 6.761 | 0.127 | 104.430 |
| 5 | 26*12 | 270 | 28.439 | 3.740 | 0.015 | 6.546 | 0.091 | 118.552 |
| 6 | | 300 | 26.139 | 3.357 | 0.015 | 6.741 | 0.124 | 131.146 |
| 7 | | 360 | 29.700 | 3.950 | 0.015 | 6.599 | 0.100 | 169.325 |
| 8 | 32*14 | 390 | 36.401 | 5.067 | 0.015 | 6.674 | 0.112 | 180.702 |
| 9 | | 420 | 37.121 | 5.187 | 0.015 | 7.134 | 0.189 | 204.874 |
| 10 | | 480 | 25.050 | 3.175 | 0.015 | 6.605 | 0.101 | 233.178 |
| 11 | 38*16 | 510 | 29.038 | 3.840 | 0.015 | 7.095 | 0.183 | 258.834 |
| 12 | | 540 | 29.726 | 3.954 | 0.015 | 6.527 | 0.088 | 272.421 |
| Average | | | | 4.090 | | | 0.132 | |

Note: gap= ($f$-LB)/LB

Table 6 lists the dispersion degree values when two assignment rules are applied to the 12 scenarios. For any car group, the ideal situation is that the developed rectangular region includes cars that are all in the same group without empty spaces or cars from other groups, i.e., the dispersion degree of each car group should be 1.0. Hence, these scenarios clearly show that the lower bound of the total dispersion degrees of the six car groups is 6.0.

As presented in Table 6, the average gap between the AR-CT solutions and the lower bound reaches approximately 4.090, verifying the development of the scattered layout of cars to be loaded onto a Ro-Ro ship. For example, in scenario 1, the total dispersion degrees of the six car groups reach approximately 31.656. For the AR-CG assignment rule, we adopt the HTSES method to obtain the layout of cars in the zone. As shown in Table 6, the average gap between the HTSES solutions and the lower bound is only approximately 0.132, which indicates the compactness of the car layout following the ship-loading process. In terms of computational performance, AR-CT is hardly time consuming because of its simplicity. Although more time is required by the HTSES, the amount is still acceptable. For example, the time required for HTSES computations is approximately 272.421 seconds when the number of cars increases to 540.

Table 7: The proportion of unassigned cars in AR-CT and AR-CG

| # | Car number | Type number | Group number | AR-CT $f$ | AR-CT $\kappa$ | AR-CG(HTSES) $f$ | AR-CG(HTSES) $\kappa$ |
|---|---|---|---|---|---|---|---|
| 11 | | 10 | | 32.394 | 0.000 | 7.142 | 0.000 |
| 12 | | 12 | | 33.644 | 0.000 | 7.168 | 0.000 |
| 13 | | 14 | | 32.893 | 0.000 | 7.259 | 0.000 |
| 14 | | 16 | | 30.873 | 0.033 | 7.081 | 0.000 |
| 15 | 180 | 18 | 6 | 32.704 | 0.056 | 7.138 | 0.000 |
| 16 | | 20 | | 34.702 | 0.122 | 7.272 | 0.000 |
| 17 | | 22 | | 34.769 | 0.128 | 7.251 | 0.000 |
| 18 | | 24 | | 33.656 | 0.139 | 7.161 | 0.000 |
| 19 | | 26 | | 36.054 | 0.211 | 7.211 | 0.000 |
| 20 | | 28 | | 36.622 | 0.239 | 7.032 | 0.000 |

Note: $\kappa$ : the proportion of unassigned cars

In AR-CT, each column in the zone can be occupied by at most two types of cars to ensure feasible car entrance and exit routes. However, as presented in Section 3.3, AR-CT is disadvantageous for the efficient use of the storage space in the zone. Table 7 presents the assignment results of AR-CT when the number of car types increases from 10 to 28. In each scenario, 180 cars are assigned to a 20*10 zone, and the number of cars of each type is generated randomly. Ideally, 20 types of cars can be assigned to a zone with 10 columns. However, because there are different numbers of cars of different types, the actual number of the assigned type is lower than this upper bound. In Table 7, we use $\kappa$ to denote the proportion of unassigned cars.

As shown in Table 7, 16 types of cars are not completely assigned to the zone in scenario 14, and the value of $\kappa$ is approximately 0.033. As the car types increase, the proportion of unassigned cars gradually increases. In scenario 20, the value of $\kappa$ is approximately 0.239. Table 7 also shows that, if AR-CG is adopted, the cars in all scenarios can be assigned to the selected zone.

Although AR-CT has obvious drawbacks, it is still applied in practice for yard management, and it can ensure feasible routes for cars entering or exiting their storage locations, even though the arrival times of cars are affected by uncertain factors. AR-CG can adapt to the detailed assignment of yard resources from the planning phase. Compared to AR-CT, it has sufficient advantages in terms of ship-loading efficiency and resource use. However, for AR-CG, addressing the unexpected factors during operation remains a challenge.

# 8. Conclusions

This paper investigates the SLAP in an automotive Ro-Ro terminal and proposes an assignment rule based on the car group. Based on the actual operational requirements, cars in the same group should be assigned to improve ship-loading efficiency as much as possible. The dispersion degree is proposed to quantify the centralized layout of car groups in the zone. We formulate a linear 0-1 integer programming model to describe the characteristics of the SLAP. The proposed model aims to minimize the total dispersion degrees of all car groups in the zone. Notably, this method avoids deadlock situations resulting from blocked car entrance and exit routes.

The attraction degree is proposed to quantitatively reflect the similarity between the location and the assigned car. Although the attraction degree illustrates only the local preference of the storage location for a car group, the CAD-CG can reflect the evolution of the car layout from scattered to centralized. Furthermore, an HTSES heuristic is developed for the car layout with the minimum dispersion degree. Finally, a rolling-horizon approach based on closed-loop feedback is presented to identify spatiotemporal conflicts between different car groups and to reduce the problem scale. Positive feedback based on guidance assignment emphasizes the guidance effect of the existing car layout in the yard on arriving cars, and negative feedback triggered by the reformulation mechanism reflects the influence of arriving cars on the existing car layout.

The first group of experiments illustrates the good performance of the HTSES and shows that it can be regarded as the basic sub method in the rolling-horizon approach. The second group of experiments, including fifteen randomly generated scenarios verifies the performance of the rolling-horizon approach. The numerical results also show that negative feedback triggered by the reformulation mechanism in the rolling approach requires a significant amount of time to analyze the conflicts over storage resources among different car groups. However, positive feedback is effective in reducing the amount of negative feedback in the rolling optimization process. Finally, based on application at the Shanghai Haitong Ro-Ro Terminal, two assignment rules, i.e., AR-CT and AR-CG, are analyzed in detail. The numerical results show that AR-CT is disadvantageous for ship-loading efficiency and the sufficient utilization of storage resources.

The SLAP presented in this paper focuses on the deterministic assignment of yard resources from the planning phase. However, during operation, the delayed arrival of cars is possible due to uncertain factors. Hence, some rescheduling strategies are necessary to adapt to uncertainty. Our future studies will focus on a stochastic programming model and a method for adjusting the car assignment plan during operation.

# Acknowledgments

This work was financially supported by the Foundation for Innovative Research Groups of the National Natural Science Foundation of China (No. 71621001), the National Natural Science Foundation of China (Nos. 72071014, 71971015, 71890972/71890970, 71525002, 71942006 and 71771016), the State key Laboratory of Rail Traffic Control and Safety (No. RCS2019ZT009), and the European Shift2Rail project OptiYard.

# References

Bergantino, A.S., Bolis, S., 2008. Monetary values of transport service attributes: land versus maritime ro-ro transport: an application using adaptive stated preferences. Maritime Policy and Management, 35(2), 159-174.

Borgman, B., Asperen, E., Dekker, R., 2010. Online rules for container stacking. OR Spectrum, 32(3), 687-716.

Cheung, R.K., Chen, C.Y., 1998. A two-stage stochastic network model and solution methods for the dynamic empty container allocation problem. Transportation Science 32(2), 142-162.

Cancı, M., and Erdal, M., 2003. *Tasimacilik Yonetimi*, 2nd ed., UTIKAD Publications, Istanbul.

Crainic, T.G., Gendreau, M., Dejax, P., 1993. Dynamic and stochastic models for the allocation of empty containers. Operations Research 41(1), 102-126.

Carlo, H.J., Vis, I.F.A., Roodbergen, K.J., 2014. Storage yard operations in container terminals: Literature overview, trends, and research directions. European Journal of Operational Research, 235(2), 412-430.

Chen, L., Lu, Z.Q., 2012. The storage location assignment problem for outbound containers in a maritime terminal. International Journal of Production Economics, 135(1), 73-80.

Cordeau, J-F., Laporte, G., Moccia, L., Sorrentino, G., 2011. Optimizing yard assignment in an automotive transshipment terminal. European Journal of Operational Research, 2011, 215(1), 149-160.

Dekker, R., Voogd, P., Eelco, V. A., 2006. Advanced methods for container stacking. OR Spectrum, 28, 563-586.

Dias, J.C.Q., Calado, J.M.F., Mendonça, M.C., 2010. The role of European «ro-ro» port terminals in the automotive supply. Journal of Transport Geography, 18(1), 116-124.

Fischer,T., Gehring, H., 2005. Planning vehicle transshipment in a seaport automobile terminal using a multi-agent system. European Journal of Operational Research, 166(3), 726-740.

Guldogan, E.U., 2010. Simulation-based analysis for hierarchical storage assignment policies in a container terminal. Simulation, 87(6), 523-537.

Han, Y., Lee, L.H., Chew, E.P., Tan, K.C., 2008. A yard storage strategy for minimizing traffic congestion in a maritime container transshipment hub. OR Spectrum, 30(4), 697-720.

Hu, Z.H., Sheng, Z.H., 2014. A decision support system for public logistics information service management and optimization. Decision Support Systems, 55(1), 219-229.

Hu, Z.H., Zhao, Y.X., Tao, S., Sheng, Z.H., 2015. Finished-vehicle transporter routing problem solved by loading pattern discovery. Annals of Operations Research, 234(1), 37-56.

Iannone, R., Miranda, S., Prisco, L., Riemma, S., Sarno, D., 2016. Proposal for a flexible discrete event simulation model for assessing the daily operation decisions in a Ro-Ro terminal. Simulation Modelling Practice and Theory, 61, 28-46.

Ishii, M., Lee, P.T.W., Tezuka, K. and Chang, Y.T., 2013. A game theoretical analysis of port competition. Transportation Research Part E, 49(1), 92-106.

Jeong, Y.H., Kim, K.H., Woo, Y.J., Seo, B.H., 2012. A simulation study on a workload-based operation planning. Industrial Engineering & Management Systems, 11(1), 103-113.

Jugovic, A., Debelic, B., Brdar, M., 2011. Short Sea Shipping in Europe Factor of the Sustainable Development Transport System of Croatia. Scientific Journal of Maritime Research, 25(1), 109-124.

Jiang, X., Lee, L.H., Chew, E.P., Han,Y., Tan, K.C., 2012. A container yard storage strategy for improving land utilization and operation efficiency in a transshipment hub port. European Journal of Operational Research, 221(1), 64-73.

Jiang, X.J., Jin, J.G., 2017. A branch-and-price method for integrated yard crane deployment and container allocation in transshipment yards. Transportation Research Part B, 98, 62-75.

Jiang, Y.N., Xu, Q., Jing, Y.Y., Jin, Z.H., 2014. Optimization of Ro-Ro ship Loading for Multiple Ports Based on Realistic Constraints. Journal of Transp. Syst. Eng. Inf. Technol, 14(1), 117-123.

Kang, J., Ryu, K.R., Kim, K.H., 2006. Deriving stacking strategies for export containers with uncertain weight information. Journal of Intelligent Manufacturing, 17(4), 399-410.

Keceli, Y., 2011. A proposed innovation strategy for Turkish port administration policy via information technology. Maritime Policy & Management, 38(2), 151-167.

Keceli, Y., Aksoy, S., Aydogdu, Y.V., 2013. A simulation model for decision support in Ro-Ro terminal operations. International Journal of Logistics Systems and Management, 15(4), 338-358.
Kim, K.H., Kim, H.B., 2002. The optimal sizing of the storage space and handling facilities for import containers. Transportation Research Part B, 36(9), 821-835.
Kim, K.H., Park, Y.M., Ryu, K-R., 2000. Deriving decision rules to locate export containers in container yards. European Journal of Operational Research, 124(1), 89-101.
Kim, K.H., Park, K.T., 2003. A note on a dynamic space-allocation method for outbound containers. European Journal of Operational Research, 148(1), 92-101.
Ku, L. P., Lee, L.H., Chew, E.P., Tan, K.C., 2010. An optimisation framework for yard planning in a container terminal: Case with automated rail-mounted gantry cranes. OR Spectrum, 32(3), 519-542.
Han, Y., Lee, L.H., Chew, E.P., Tan, K.C., 2008. A yard storage strategy for minimizing traffic congestion in a maritime container transshipment hub. OR Spectrum, 30(4), 697-720.
Laik, N., Hadjiconstantinou, E., 2008. Container assignment and gantry crane deployment in a container terminal: A case study. Maritime Economics & Logistics, 10(1-2), 90-107.
Lee, L.H., Chew, E.P., Tan, K.C., Han, Y, 2007. An optimization model for storage yard management in transshipment hubs. Container Terminals and Cargo Systems: Design, Operations Management, and Logistics Control Issues, 107-129.
Lee, D.H., Jin, J.G., Chen, J.H., 2012a. Schedule template design and storage allocation for cyclically visiting feeders in container transshipment hubs. Transportation Research Record, 2273, 87-95.
Lee, D.H., Jin, J.G., Chen, J.H., 2012b. Terminal and yard allocation problem for a container transshipment hub with multiple terminals. Transportation Research Part E, 48(2), 516-528.
Lee, L.H., Chew, E.P., Tan, K.C., Han, Y., 2006. An optimization model for storage yard management in transshipment hubs. OR Spectrum, 28, 539-561.
Liu, C.C., Zhang, C.R., Zheng, L., 2017. A bi-objective model for robust yard allocation scheduling for outbound containers. Engineering Optimization, 49(1), 113-135.
Mangan, J., Lalwani, C., Gardner, B., 2002. Modelling port/ferry choice in Ro-Ro freight transportation. International Journal of Transport Management, 1(1), 15-28.
Maksimavicius, R.,2004. Some elements of the Ro-Ro terminals. Transport, 2(19), 75-81.
Mattfeld, D.C., Kopfer, H., 2003. Terminal operations management in vehicle transshipment. Transportation Research Part A, 37(6), 435-452.
Mattfeld, D.C., Orth, H., 2006. The allocation of storage space for transshipment in vehicle distribution. OR spectrum, 28(4), 681-703.
Morales-Fusco, P., Saurí, S., Spuch, B., 2010. Quality indicators and capacity calculation for Ro-Ro terminals. Transportation Planning and Technology, 33(8), 695-717.
Morales-Fusco, P., Saurí, S., Lago, A., 2012. Potential freight distribution improvements using motorways of the sea. Journal of Transport Geography, 24,1-11.
Murty, K.G., Liu, J., Wan, Y.W., Linn, R., 2005. A decision support system for operations in a container terminal. Decision Support Systems, 39(3), 309-332.

Murty, K.G., Wan, Y.W., Liu, J., Tseng, M.M., Leung, E., Lai, K.K., Chiu, W.C., 2005. Hong Kong International Terminals gains elastic capacity using a data-intensive decision-support system. Interfaces, 35(1), 61-75.

Ng, W. C., Mak, K.L., Li, M.K., 2010. Yard planning for vessel services with a cyclical calling pattern. Engineering Optimization, 42(11), 1039-1054.

Nishimura, E., Imai, A., Janssens, G. K., Papadimitriou, S., 2009. Container storage and transshipment marine terminals. Transportation Research Part E, 45(5), 771-786.

Özkan, E. D., Nas, S., Güler, N., 2016. Capacity Analysis of Ro-Ro Terminals by Using Simulation Modeling Method. The Asian Journal of Shipping and Logistics, 32(3), 139-147.

Park, T., Choe, R., Kim, Y.H., and Ryu, K.R., 2011. Dynamic adjustment of container stacking policy in an automated container terminal. International Journal of Production Economics, 133(1), 385-392.

Preston, P., Kozan, E., 2001. An approach to determine storage locations of containers at seaport terminals. Computers & Operations Research, 28(10), 983-995.

Wang, X., F., Chen, K., 2013. Ro-Ro terminals. Shang Hai Jiao Tong University.

Shen, W.S., Khoong, C.M., 1995. A DSS for empty container distribution planning. Decision Support Systems, 15(1), 75-82.

Sharif, O., Huynh, N., 2013. Storage space allocation at marine container terminals using ant-based control. Decision Support Systems, 40(6), 2323-2330.

Stahlbock, R., Voß, S., 2008. Operation research at container terminals: a literature update. OR Spectrum, 30(1), 1-52.

Steenken, D., Voß, S., Stahlbock, R., 2004. Container terminal operation and operations research - a classification and literature review. OR spectrum, 26(1), 2-49.

Vilkelis, A., Jakovlev, S., 2014. Outbound supply chain collaboration modelling based on the automotive industry. Transport, 29(2), 223-230.

Woo, Y. J., Kim, K.H., 2011. Estimating the space requirement of outbound container inventories in port container terminals. International Journal of Production Economics, 133(1), 293-301.

Wu, H.R., Zhu, X.N., 2015. Container Slot Allocation Model of Mixed Storage in "Ships, Yard, Trains" Yard. Journal of Transp. Syst. Eng. Inf. Technol, 15(4), 198-203.

Yu, M., Qi, X., 2013. Storage space allocation models for inbound containers in an automatic container terminal. European Journal of Operational Research, 2013, 226(1), 32-45.

Zeng, Q.C., Li, H.Y., Wu, P., 2017. Re-handling Strategies for Import Containers Based on Partial Truck Arrival Information in Container Terminals. Journal of Transp. Syst. Eng. Inf. Technol, 17(1), 191-198.

Zhou, S.F., Zhang, Q.N., 2018. Container Storage Strategies Research Based on Synchronization of Customers' Retrieval Processes. Journal of Transp. Syst. Eng. Inf. Technol, 18(5), 151-157.

Zhang, C., Liu, J., Wan, Y-W., Murty, K.G., Linn, R.J., 2003. Storage space allocation in container terminals. Transportation Research Part B, 37(10), 883-903.

# Appendix: Symbols and pseudocode

## I. Symbols and pseudocode in the HTSES

**(a) Symbols:**

| | |
|---|---|
| $\Gamma$ | Car layout |
| $\Gamma^*$ | Ideal car layout |
| $f$ | Total dispersion degrees in car layout $\Gamma$ |
| $f^*$ | Total dispersion degree in car layout $\Gamma^*$ |
| $L$ | Set that records the assigned location of each car and its group, i.e., $L = \{(u,(r,c),g) \mid x_u^{(r,c)} = 1, B_{g,u} = 1, u \in U, g \in G, r \in R, c \in C\}$. |
| $l_{(r,c)}^g$ | Attraction degree of location $(r,c)$ for cars in group-*g* |
| $\psi_{(r,c)}$ | Neighborhood space of location $(r,c)$ in the selected zone/zones |
| $J_{\hat{g}}$ | Set that records the attraction degree of each location in group- $\hat{g}$ , i.e., $J_{\hat{g}} = \{((r,c), l_{(r,c)}^{\hat{g}}) \mid r \in R, c \in C\}$ |
| $\mathscr{L}_g$ | Cumulative attraction degrees of group-*g*, i.e., $\mathscr{L}_g = \sum_{u \in U} \sum_{r \in R} \sum_{c \in C} x_u^{(r,c)} \cdot B_{g,u} \cdot l_{(r,c)}^g$ |
| $\mathscr{L}$ | Total cumulative attraction degrees, i.e., $\mathscr{L} = \sum_{g \in G} \mathscr{L}_g$ |
| $\mathscr{L}^*$ | Maximum total cumulative attraction degrees |

**(b) Pseudocode:**

**Input:** The groups, arrival and departure sequences of cars

**Initialize**: Randomly assign all cars to the selected zone/zones, formulate the initial car layout $\Gamma$ , and calculate the values of $f$ and $l_{(r,c)}^g$ ( $g \in G$; $r \in R$; $c \in C$ ).
Initially, $\Gamma^* \Leftarrow \Gamma$, and $f^* \Leftarrow f$ .

***The first stage: maximize the total CAD_CG ( $\mathscr{L}$ ).***

Formulate set $L$ and calculate the value of $\mathscr{L}$ . Initially, $\mathscr{L}^* \Leftarrow \mathscr{L}$ .

**While** ( $L \neq \varnothing$ ), **do**

Select $(\hat{u},(\hat{r},\hat{c}),\hat{g}) = Arg \min_{u,(r,c),g} \{l_{(r,c)}^g \mid (u,(r,c),g) \in L\}$ and formulate set $J_{\hat{g}}$ ;

**While** ( $J_{\hat{g}} \neq \varnothing$ ), **do**

Select $(\tilde{r},\tilde{c}) = Arg \max_{(r,c)} \{l_{(r,c)}^{\hat{g}} \mid ((r,c), l_{(r,c)}^{\hat{g}}) \in J_{\hat{g}}\}$ ;

Move or exchange the cars in locations $(\hat{r},\hat{c})$ and $(\tilde{r},\tilde{c})$ to obtain new car layout $\Gamma'$ ;
Calculate the values of $\mathscr{L}'$ and $f'$ in $\Gamma'$ .

**If** $\mathscr{L}' > \mathscr{L}^*$ , **then**

$\mathscr{L}^* \Leftarrow \mathscr{L}'$, and $\Gamma^* \Leftarrow \Gamma'$, and $f^* \Leftarrow f'$; **break;**

**Otherwise,** $((\tilde{r},\tilde{c}), l^{\hat{g}}_{(\tilde{r},\tilde{c})})$ is removed from set $J_{\hat{g}}$.

**End if**

**End while**

**If** the better car layout is obtained, **then**

update the value of $x_u^{(r,c)}$ and $l^g_{(r,c)}$; and update set $L$.

**Otherwise,** $(\hat{u},(\hat{r},\hat{c}),\hat{g})$ is removed from set $L$.

**End if**

**End while**

***End the first stage***

***The second stage: minimize the total dispersion degrees of all car groups***

Calculate the value of $f^*$ in $\Gamma^*$ ($f^* = \sum_{g \in G} f_g^*$).

$g = 1$

**While** ($g < |G|$), **do**

Formulate the compaction, unsaturated and neighborhood regions for group-*g* cars in $\Gamma^*$.

Move the group-*g* cars in the unsaturated region into each neighborhood region and formulate new car layout $\Gamma'$.

Calculate the value of $f'$ in $\Gamma'$;

**If** $f' < f^*$, **then** $\Gamma^* \Leftarrow \Gamma'$, and $f^* \Leftarrow f'$, and update the value of $x_u^{(r,c)}$; $g = 1$.

**Otherwise**, $g \Leftarrow g+1$.

**End if**

**End while**

**End the second stage**

**Output:** ideal car layout $\Gamma^*$ and total dispersion degree $f^*$.

## II. Symbols and pseudocode for the rolling-horizon approach

**(a) Symbols:**

| | |
|---|---|
| $T$ | Set of discretized time steps (sequences), indexed by $T_s$, i.e., $T = \{T_1, \ldots, T_s, \ldots, T_n\}$ |
| $V_s$ | Set of departure (loaded) cars at each discrete time $T_s$, i.e., $V_s = \{u \mid t_u^a = T_s, u \in U\}$ |
| $U_s$ | Set of arriving cars at time region $[T_{s-1}, T_s)$, i.e., $U_s = \{u \mid T_{s-1} \le t_u^a < T_s, u \in U\}$ |
| $W_s$ | Set of existing cars in the selected zone/zones at time region $[T_{s-1}, T_s]$, i.e., $W_s = \{u \mid u \in U, t_u^a < T_{s-1}, t_u^d > T_{s-1}\}$ |
| $K$ | Temporary car set |
| $\Gamma_s$ | Car layout at time $T_s$ |

| | |
|---|---|
| $f_s$ | Total dispersion degrees of departing car groups at time $T_s$ |
| $\hat{\Gamma}_s$ | Car layout obtained by the positive feedback at time $T_s$ |
| $\hat{f}_s$ | Total dispersion degrees of departing car groups at time $T_s$ in the positive feedback process |
| $\tilde{\Gamma}_s$ | Reformulated car layout obtained by the negative feedback at time $T_s$ |
| $\tilde{f}_s$ | Total dispersion degrees of departing car groups at time $T_s$ in the negative feedback process |

1 **(b) Pseudocode:**

**Input:** All assigned cars in the yard and their groups and arrival and departure times.

**Initialize**: Formulate discrete time set $T$ ($T = \{T_1, \ldots, T_s, \ldots, T_n\}$) based on the departure times (loading sequences) of cars, and determine set $U_s$, $V_s$, and $W_s$.

Adopt the ***HTSES*** to assign the cars in set $U_1$ and formulate car layout $\Gamma_1$ at time $T_1$.

**While** ( $s < n$ ), **do**

Remove the cars in set $V_s$ from $\Gamma_s$;

***The positive feedback based on the guidance mechanism****:*

Formulate set $K$, and $K \Leftarrow U_{s+1}$.

**While** ( $K \neq \varnothing$ ), **do**

Select car $\hat{u}$ in set $K$ and calculate the value of $l_{(r,c)}^{\hat{g}}$ based on its group $\hat{g}$;

the guidance assignment mechanism based on the attraction degree **(GAM_AD)**:

Assign car $\hat{u}$ to location $(\hat{r}, \hat{c})$,

$(\hat{r}, \hat{c}) = Arg \max_{(r,c)} \{ l_{(r,c)}^{\hat{g}} \mid \exists\, v \in W_{s+1},\ x_v^{(r,c)} = 0, r \in R, c \in C \}$;

Car $\hat{u}$ is removed from set $K$.

**End while**

Obtain car layout $\hat{\Gamma}_{s+1}$;

Adopt the ***HTSES*** to improve $\hat{\Gamma}_{s+1}$;

Calculate the value of $\hat{f}_{s+1}$ in $\hat{\Gamma}_{s+1}$.

***End the positive feedback process***

**Layout reformulation for the cars in set** $U_{s+1}$ **and** $W_{s+1}$ **:**

Adopt the ***HTSES*** to reformulate the car layout for the cars in sets $U_{s+1}$ and $W_{s+1}$, obtain car layout $\tilde{\Gamma}_{s+1}$, and calculate the value of $\tilde{f}_{s+1}$;

***Identification of the efficient reformulation****:*

**If** $\hat{f}_{s+1} > \tilde{f}_{s+1}$**, then**

**Negative feedback based on the reformulation mechanism**:

$s' = s+1$

**While (** $s' \geq 1$ **), do**

Remove the cars in set $U_{s'}$ from $\tilde{\Gamma}_{s'}$;

Adopt the ***GAM_AD*** and ***HTSES*** for the cars in set $V_{s'}$, formulate car layout $\tilde{\Gamma}_{s'}$ at time $T_{s'}$, and calculate the total dispersion degrees of departing car groups ( $\tilde{f}_{s'}$ ).

$s' \Leftarrow s' - 1$;

**End while**

**If** $\sum_{k=1}^{s-1} \tilde{f}_k + \tilde{f}_s < \sum_{k=1}^{s-1} f_k + \hat{f}_s$**, then**

Negative feedback is efficient, and the reformulated car layout from $s' = 1$ to $s+1$ is accepted, i.e., $\Gamma_{s'} \Leftarrow \tilde{\Gamma}_{s'}$ and $f_{s'} \Leftarrow \tilde{f}_{s'}$ ( $s' = 1,\ 2,\ \cdots,\ s+1$ ).

**Otherwise,** $\Gamma_s \Leftarrow \hat{\Gamma}_s$ and $f_s \Leftarrow \hat{f}_s$.

**End If**

***End the negative feedback process***

**Otherwise,** $\Gamma_s \Leftarrow \hat{\Gamma}_s$ and $f_s \Leftarrow \hat{f}_s$.

**End If**

***End the identification of the car layout reformulation***

$s \Leftarrow s+1$

**End while**

**Output:** car layout $\Gamma_s$ and dispersion degree $f_s$ ( $s = 1,\ 2,\ \cdots,\ n$ ).